

$N < 4$ On-Shell Diagrams

Taro V. Brown^a

^a*Department of Physics, UC Davis, One Shields Avenue, Davis, CA 95616, USA*

E-mail: tvbrown@ucdavis.edu

ABSTRACT: Using on-shell diagrams we calculate various amplitudes in $\mathcal{N} = 4$. We then extend this to $\mathcal{N} \neq 4$ focusing on $\mathcal{N} = 0$ and analyze the singularity structure of the results. Finally we calculate higher loop forms at five points.

Contents

1	Introduction	2
2	Grassmannian	2
3	Introduction to on-shell diagrams	4
3.1	Three point on-shell form	4
3.2	Four-point directly from $G(2,4)$ matrix	7
3.2.1	Using face-variables	7
3.2.2	Using edge-variables	10
4	Examples of on-shell diagrams at five and six points	12
4.1	Five point	12
4.2	Six-point NMHV	13
5	Calculating $\mathcal{N} < 4$ amplitudes	16
5.1	The measure	16
5.2	Four-point $\mathcal{N} = 0$ with internal loop	16
5.3	Five-point $\mathcal{N} = 0$, no internal cycle	17
5.4	Five point with internal cycles	18
5.5	Six-point $\mathcal{N} = 0$	20
5.6	Six point NMHV with internal cycles	21
5.7	Singularities	23
6	Higher loops	25
6.1	2 loop four-point	25
6.2	Three loop five-point in $\mathcal{N} = 0$, no internal cycle	25
6.3	Three loop five-point in $\mathcal{N} = 0$ with internal cycle	27
6.4	Singularities	29
7	Summary and outlook	31

1 Introduction

During the last few decades, significant strides have been made in the study of scattering amplitudes. New modern on-shell techniques have made calculations with a large number of particles and loops feasible. Many of the significant advancements in the field has come by studying $\mathcal{N} = 4$ super Yang-Mills (sYM) and using its planar, or large N , limit as a sandbox to explore the underlying geometric structure [1–5].

In recent years this geometric structure of scattering amplitudes in $\mathcal{N} = 4$ sYM has been explored using the positive Grassmannian, on-shell diagrams, and the Amplituhedron [6–8]. A natural progression is to try and extend these discoveries beyond planar $\mathcal{N} = 4$ sYM to explore whether the geometric interpretation is a more general feature of quantum field theories (QFTs). Similarly, considering theories with $\mathcal{N} \neq 4$, such as supergravity ($\mathcal{N} = 8$), will teach us to what extent these geometric pictures apply to other field theories.

The focus of this project has been some of these extensions, with the report structured as follows. In section 2 we give a short review of the Grassmannian, followed by an introduction to on-shell diagrams. Then, in sections 3 and 4 we calculate various examples using the methods described. We extend this approach to theories for $\mathcal{N} \neq 4$ in section 5, focusing on $\mathcal{N} = 0$ ¹, explicitly calculating multiple examples at five and six points. Then diagrams at higher loops are considered in section 6 and finally we consider the singularity structure of the results found.

2 Grassmannian

In this section we give a brief review of the Grassmannian, which will serve as a crucial ingredient for our discussion of on-shell diagrams. The Grassmannian, denoted $G(k, n)$, is the space of k -planes going through the origin in n dimensions. It can be thought of as a generalization of projective space P^{n-1} , which is the space of lines going through the origin in n -dimensions, since $G(1, n) = P^{n-1}$. One can e.g. take k vectors in n dimensions, see figure 2

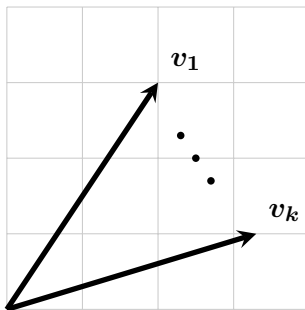


Figure 1. k n -dimensional vectors going through the origin

¹The results found at $\mathcal{N} = 0$ can easily be extended by adding super momentum delta functions in the calculation.

The span of these vectors gives the k - plane. If they are stacked, we get a matrix $C_{\alpha a}$

$$k \begin{bmatrix} V_1 \\ \vdots \\ V_k \end{bmatrix} \equiv C_{\alpha a}, \quad \alpha = 1, \dots, k \quad a = 1, \dots, n \quad (2.1)$$

This matrix is generally not unique since it has a $GL(k)$ redundancy, $C_{\alpha a} \sim L_{\alpha}^{\beta} C_{\beta a}$. The dimensionality of the Grassmannian is

$$\dim G(k, n) = \overbrace{k \times n}^{k \times n \text{ matrix}} \underbrace{-k^2}_{GL(k) \text{ red}} \quad (2.2)$$

The redundancy means that we can gaugefix the matrix using a linear transformation by setting any $k \times k$ blok to the identity. This is equivalent to the rescaling of a vector in projective space to $\begin{pmatrix} 1 & v_2 & v_3 & v_4 & \dots \end{pmatrix}$. Taking e.g. $G(3, 5)$, we have six degrees of freedom:

$$G(3, 5) = \left[\begin{array}{ccc|cc} 1 & 0 & 0 & x_4 & x_5 \\ 0 & 1 & 0 & y_4 & y_5 \\ 0 & 0 & 1 & z_4 & z_5 \end{array} \right] \quad (2.3)$$

The dimensionality of the Grassmannian is symmetric under $n \leftrightarrow k$. This is because there is a bijection between the Grassmania: k and $n - k$ planes in n dimensions, since these planes are orthogonal. In the case above C^{\perp} is a 2-plane in 5 dimensions. We can illustrate both the matrices like so,

$$\left[\begin{array}{ccc|cc} 1 & 0 & 0 & x_4 & x_5 \\ 0 & 1 & 0 & y_4 & y_5 \\ 0 & 0 & 1 & z_4 & z_5 \\ \hline -x_4 & -y_4 & -z_4 & 1 & 0 \\ -x_5 & -y_5 & -z_5 & 0 & 1 \end{array} \right] \quad (2.4)$$

With the bottom part just being the negative transpose of the x, y and z coordinates in the upper right corner. The invariants are determinants of any k minors, labeling these by their indices:

$$\begin{pmatrix} a_1 & a_2 & \dots & a_k \end{pmatrix} \quad (2.5)$$

We will now proceed to use the properties of the Grassmannian by introducing the concept of on-shell diagrams.

3 Introduction to on-shell diagrams

In this section we introduce the notion of on-shell diagrams, and give examples on different ways one can calculate differential forms from these.

One can construct $(k \times n)$ C-matrices out of on-shell diagrams, where k labels the number of negative helicity particles and n is the total number of particles. The procedure to construct a matrix from a diagram using *edge-variables* is as follows

- Label the edges of the on-shell diagram by α 's. Not all edges have to be labeled due to the $GL(k)$ redundancy.
- Starting at one of the incoming particles (say, 2), trace a path to one of the outgoing particles (say, 4). Multiply the α 's encountered on the path. This would be entry C_{24} in the C-matrix, i.e.

$$C_{ab} = \sum_{\Gamma(a \rightarrow b)} \prod_j \alpha_j \quad (3.1)$$

- When going from an incoming particle to another incoming particle, put a 0 in that matrix entry, unless it is a path starting and ending at the same particle, then put a 1.
- If the path encounters an internal cycle that forms a complete loop, the matrix element is multiplied by the geometric series, labeled by δ , containing the edge-variables encountered in that loop, i.e.

$$\delta = \sum_{n=0}^{\infty} (\alpha_i \alpha_j \alpha_k \cdots)^n = \frac{1}{1 - (\alpha_i \alpha_j \alpha_k \cdots)} \quad (3.2)$$

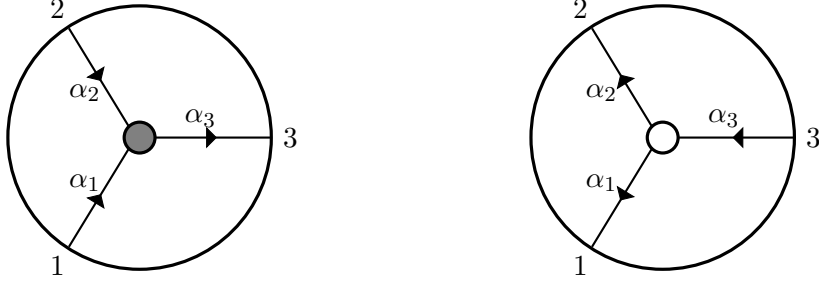
- The form is then found through

$$d\Omega = \prod_{i=1}^N \frac{d\alpha_i}{\alpha_i} \delta(C \cdot Z) \mathcal{J}^{\mathcal{N}-4} \quad (3.3)$$

where $\delta(C \cdot Z) \equiv \delta(C \cdot \tilde{\lambda}) \delta(C^\perp \cdot \lambda) \delta(C \cdot \tilde{\eta})$, and \mathcal{J} is a Jacobian which we will describe in further detail in section 5. We will now calculate amplitudes through various techniques using the on-shell diagrams.

3.1 Three point on-shell form

The easiest example is the two diagrams representing the three-point MHV and $\overline{\text{MHV}}$ amplitudes in $\mathcal{N} = 4$ sYM. Taking e.g the amplitudes to be $A_3^{\text{MHV}}(1^-, 2^-, 3^+)$ and $A_3^{\overline{\text{MHV}}}(1^+, 2^+, 3^-)$, the on-shell diagrams are



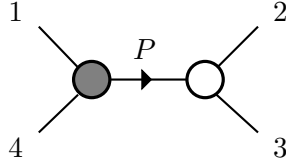
These produce the two following C matrices, respectively

$$C = \begin{pmatrix} 1 & 0 & \alpha_1 \alpha_2 \\ 0 & 1 & \alpha_2 \alpha_3 \end{pmatrix}, \quad C = \begin{pmatrix} \alpha_1 \alpha_3 & \alpha_2 \alpha_3 & 1 \end{pmatrix} \quad (3.4)$$

The amplitudes in this case are

$$\begin{aligned} A_3^{\text{MHV}}(1, 2, 3) &= \frac{\delta(\mathcal{Q}) \delta(P)}{\langle 12 \rangle \langle 23 \rangle \langle 31 \rangle} \\ A_3^{\overline{\text{MHV}}}(1, 2, 3) &= \frac{\delta([12] \tilde{\eta}_3 + [23] \tilde{\eta}_1 + [31] \tilde{\eta}_2) \delta(P)}{[12][23][31]} \end{aligned} \quad (3.5)$$

where $\mathcal{Q} \equiv \sum_{i=1}^3 \lambda_i \tilde{\eta}_i$ and $P \equiv \sum_{i=1}^3 \lambda_i \tilde{\lambda}_i$. One can further construct more elaborate diagrams by gluing these three point functions together. The simplest possible diagram, found by stitching together two vertices of opposite helicity ($k = 1$ and $k = 2$), is shown below



To construct the four-point diagram we then glue the two three-point amplitudes together by integrating over the internal degrees of freedom through

$$\prod_I \int d^4 \tilde{\eta}_I \int \frac{d^2 \lambda_I d^2 \tilde{\lambda}_I}{GL(1)} \quad (3.6)$$

Explicitly we have

$$\begin{aligned} \int d\tilde{\eta}_P \int \frac{d^2 \lambda_P d^2 \tilde{\lambda}_P}{GL(1)} & \frac{\delta^8(\lambda_1 \tilde{\eta}_1 + \lambda_4 \tilde{\eta}_4 + \lambda_P \tilde{\eta}_P) \delta^4(\lambda_1 \tilde{\lambda}_1 + \lambda_4 \tilde{\lambda}_4 + \lambda_P \tilde{\lambda}_P)}{\langle 14 \rangle \langle 4P \rangle \langle P1 \rangle} \\ & \times \frac{\delta^4([23] \tilde{\eta}_P + [3P] \tilde{\eta}_2 + [P3] \tilde{\eta}_3) \delta^4(\lambda_2 \tilde{\lambda}_2 + \lambda_3 \tilde{\lambda}_3 - \lambda_P \tilde{\lambda}_P)}{[23][3P][P2]} \end{aligned} \quad (3.7)$$

First we solve the delta-function constraint by projecting along λ_1

$$\begin{aligned}\lambda_1 \tilde{\lambda}_1 + \lambda_4 \tilde{\lambda}_4 + \lambda_P \tilde{\lambda}_P &= 0 \\ \Rightarrow \tilde{\lambda}_P &= \frac{\langle 41 \rangle}{\langle 1P \rangle} \tilde{\lambda}_4.\end{aligned}\tag{3.8}$$

Similarly we use the other delta-function and project using $\tilde{\lambda}_3$

$$\begin{aligned}\lambda_2 \tilde{\lambda}_2 + \lambda_3 \tilde{\lambda}_3 - \lambda_P \tilde{\lambda}_P &= 0 \\ \Rightarrow \lambda_P &= \frac{[23]}{[P3]} \lambda_2.\end{aligned}\tag{3.9}$$

Combining these we obtain

$$\begin{aligned}\tilde{\lambda}_P \lambda_P &= \lambda_2 \tilde{\lambda}_4 \frac{\langle 41 \rangle [23]}{\langle 1P \rangle [P3]} = \lambda_2 \tilde{\lambda}_4 \frac{[23]}{[43]} \\ &= \lambda_2 \tilde{\lambda}_4 \frac{\langle 41 \rangle}{\langle 12 \rangle}\end{aligned}\tag{3.10}$$

where we have used $P = -1 - 4 = 2 + 3$ in the last two equalities. Solving this collapses the momentum conservation delta function as well as giving a Jacobian factor of $\frac{1}{\langle 23 \rangle [32]}$

$$\begin{aligned}\lambda_P &= \lambda_2 \\ \tilde{\lambda}_P &= \lambda_4 \frac{\langle 41 \rangle}{\langle 12 \rangle} = \tilde{\lambda}_4 \frac{[23]}{[43]}\end{aligned}\tag{3.11}$$

We then use these in one of the grassmann delta-functions

$$\begin{aligned}\tilde{\eta}_P &= \frac{-[3P]\tilde{\eta}_2 - [P2]\tilde{\eta}_3}{[23]} \\ &= -\frac{1}{[23]} \times \frac{[34][23]}{[43]} \times \tilde{\eta}_2 - \frac{1}{[23]} \times \frac{[42]\langle 41 \rangle}{\langle 12 \rangle} \times \tilde{\eta}_3 \\ &= \tilde{\eta}_2 + \frac{\langle 13 \rangle}{\langle 12 \rangle} \times \tilde{\eta}_3\end{aligned}\tag{3.12}$$

This can be obtained from contracting

$$\lambda_P \tilde{\eta}_P = \lambda_2 \tilde{\eta}_2 + \lambda_3 \tilde{\eta}_3\tag{3.13}$$

with λ_1 , since $\lambda_P = \lambda_2$. Using this in the other grassmann delta function we get $[23]^4 \delta^8(\sum_i \lambda_i \tilde{\eta}_i)$. Finally we take the solutions (3.11) and insert them into the bosonic delta-function

$$\begin{aligned}0 &= \lambda_1 \tilde{\lambda}_1 + \lambda_4 \tilde{\lambda}_4 + \lambda_P \tilde{\lambda}_P = \lambda_1 \tilde{\lambda}_1 + \tilde{\lambda}_4 \left(\lambda_4 + \lambda_2 \frac{[23]}{[43]} \right) \\ &= \lambda_1 \tilde{\lambda}_1 + \tilde{\lambda}_4 \left(\frac{\lambda_4 [43] + \lambda_2 [23]}{[43]} \right) = \lambda_1 \left(\tilde{\lambda}_1 + \tilde{\lambda}_4 \frac{[13]}{[34]} \right) \\ &= \lambda_1 \left(\frac{\tilde{\lambda}_1 [34] + \tilde{\lambda}_4 [13]}{[34]} \right) = \lambda_1 \tilde{\lambda}_3 \frac{[14]}{[34]}\end{aligned}\tag{3.14}$$

Since $\lambda_1 \neq 0$, and $\tilde{\lambda}_3 \neq 0$ this leads to $[14] = 0$ which in turn gives us

$$(p_1 + p_4)^2 = \langle 14 \rangle [41] = 0 \quad (3.15)$$

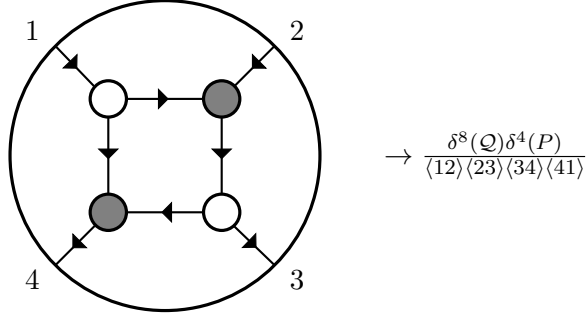
Now we only need the kinematic part of the integrand. Including the Jacobians and using $\langle 1P \rangle [P3] = \langle 12 \rangle [23]$ and $\langle 4P \rangle [P2] = \langle 43 \rangle [32]$ we obtain

$$\frac{1}{\langle 14 \rangle \langle 4P \rangle \langle P1 \rangle} \times \frac{1}{[23][3P][P2]} \times \frac{[23]^4}{\langle 23 \rangle [23]} = \frac{1}{\langle 12 \rangle \langle 23 \rangle \langle 34 \rangle \langle 41 \rangle} \quad (3.16)$$

Such that we in total have the form

$$\frac{\delta^8(Q) \delta^4(P)}{\langle 12 \rangle \langle 23 \rangle \langle 34 \rangle \langle 41 \rangle} \delta((p_1 + p_4)^2) \quad (3.17)$$

This is not surprising since the diagram we considered is not a Feynman diagram. Rather the first diagram to give the four-point on-shell amplitude arises from gluing 4 three-point functions together



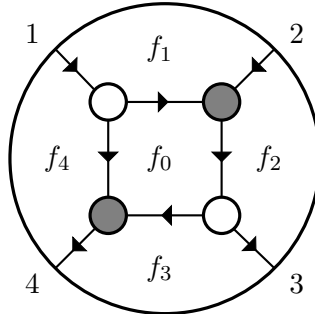
In the next section we will present two methods of getting the amplitude directly from the diagram.

3.2 Four-point directly from $G(2, 4)$ matrix

The calculation of the C -matrix can be performed either using face or edge variables. We are going to show how to do both for good measure.

3.2.1 Using face-variables

The four-point diagram with face-variables looks like this



While the C -matrix is found through

$$C_{ab} = - \sum_{\Gamma(a \rightarrow b)} \prod_j (-f_j), \quad \text{on the right} \quad (3.18)$$

with the added constraint

$$\prod_j f_j = -1 \quad (3.19)$$

Using the above, we find the matrix to have the following entries

$$C = \begin{pmatrix} 1 & 0 & f_0 f_3 f_4 & f_4(1 - f_0) \\ 0 & 1 & -f_0 f_1 f_3 f_4 & f_0 f_1 f_4 \end{pmatrix} \quad (3.20)$$

Note that f_2 doesn't appear, which means that according to (3.19) we can take the remaining f 's as independent. Positivity (all minors are positive) then demands that

$$f_0 < 0, \quad f_1 > 0, \quad f_2 < 0, \quad f_3 < 0, \quad (3.21)$$

While the perpendicular C -matrix satisfying $C \cdot C^\perp = 0$ is easily obtained

$$C^\perp = \begin{pmatrix} -f_0 f_3 f_4 & f_0 f_1 f_3 f_4 & 1 & 0 \\ -f_4(1 - f_0) & -f_0 f_1 f_4 & 0 & 1 \end{pmatrix} \quad (3.22)$$

we can then find the form through

$$d\Omega = \frac{df_0}{f_0} \frac{df_1}{f_1} \frac{df_3}{f_3} \frac{df_4}{f_4} \delta(C \cdot \tilde{\lambda}) \delta(C^\perp \cdot \lambda) \delta(C \cdot \tilde{\eta}) \quad (3.23)$$

First let us look at the delta-functions, such that we can specify the face-variables in terms of the spinor products. We start by looking at $\lambda \cdot C^\perp = 0$, from which we get two equations

$$C^\perp \cdot \lambda = 0 \Rightarrow \begin{cases} -\lambda_1 f_0 f_3 f_4 + \lambda_2 f_0 f_1 f_3 f_4 + \lambda_3 & = 0 \\ -\lambda_1 f_4(1 - f_0) - \lambda_2 f_0 f_1 f_4 + \lambda_4 & = 0 \end{cases} \quad (3.24)$$

By multiplying the first equation by λ_2 one obtains $f_0 f_3 f_4 = -\frac{\langle 23 \rangle}{\langle 12 \rangle}$. Similarly multiplying the second equation by λ_1 we get $f_0 f_1 f_4 = \frac{\langle 14 \rangle}{\langle 12 \rangle}$. Combining these two,

$$f_1 = -\frac{\langle 14 \rangle}{\langle 23 \rangle} f_3 \quad (3.25)$$

Then multiplying the first equation by $\tilde{\lambda}_1$ we have $f_0 f_1 f_3 f_4 = -\frac{\langle 13 \rangle}{\langle 12 \rangle}$ together with the previous result, this leads to

$$f_3 = -\frac{\langle 13 \rangle}{\langle 14 \rangle} \quad \text{and} \quad f_1 = \frac{\langle 13 \rangle}{\langle 23 \rangle} \quad (3.26)$$

The other equations are solved similarly and we obtain

$$\begin{aligned} f_0 &= -\frac{\langle 14 \rangle \langle 23 \rangle}{\langle 12 \rangle \langle 34 \rangle} \\ f_4 &= -\frac{\langle 34 \rangle}{\langle 13 \rangle} \end{aligned} \quad (3.27)$$

Let us now evaluate the two remaining delta-functions. From $C \cdot \tilde{\lambda}$ we get two equations.

$$0 = \tilde{\lambda}_1 + f_0 f_3 f_4 \tilde{\lambda}_3 + f_4 (1 - f_0) \tilde{\lambda}_4 = \tilde{\lambda}_1 + \frac{\langle 32 \rangle}{\langle 12 \rangle} \tilde{\lambda}_3 + \frac{\langle 42 \rangle}{\langle 12 \rangle} \tilde{\lambda}_4 \quad (3.28)$$

and

$$0 = \tilde{\lambda}_2 + \frac{\langle 13 \rangle}{\langle 12 \rangle} \tilde{\lambda}_3 + \frac{\langle 14 \rangle}{\langle 12 \rangle} \tilde{\lambda}_4 \quad (3.29)$$

where we have used a Schouten identity for the coefficient of $\tilde{\lambda}_4$

$$\langle 41 \rangle \langle 23 \rangle + \langle 12 \rangle \langle 34 \rangle = \langle 13 \rangle \langle 24 \rangle \quad (3.30)$$

We see that these equations can all be obtained from a momentum conservation delta-function by contracting it with λ_1 and λ_2

$$\delta^4(\lambda_1 \tilde{\lambda}_1 + \lambda_2 \tilde{\lambda}_2 + \lambda_3 \tilde{\lambda}_3 + \lambda_4 \tilde{\lambda}_4) \equiv \delta^4(P) \quad (3.31)$$

For the last delta-function we get the exact same thing except for replacing $\tilde{\lambda}_i \rightarrow \tilde{\eta}_i$

$$\delta^8(\lambda_1 \tilde{\eta}_1 + \lambda_2 \tilde{\eta}_2 + \lambda_3 \tilde{\eta}_3 + \lambda_4 \tilde{\eta}_4) \equiv \delta^8(\mathcal{Q}) \quad (3.32)$$

Note that we get an extra factor of $\frac{1}{\langle 12 \rangle^4}$ from re-writing the delta-functions by projecting along λ_1 and λ_2 . Finally we get a Jacobian from solving the delta-function constraints

$$J = |J_{ij}| = f_0^2 f_1 f_3 f_4^3 = \frac{\langle 23 \rangle \langle 34 \rangle \langle 41 \rangle}{\langle 12 \rangle^2 \langle 13 \rangle} \quad (3.33)$$

where

$$J_{ij} = \frac{\partial E_i}{\partial f_j} = \begin{pmatrix} f_3 f_3 & 0 & f_0 f_3 & f_0 f_4 \\ f_1 f_3 f_4 & f_0 f_3 f_4 & f_0 f_1 f_4 & f_0 f_1 f_3 \\ f_4 & 0 & 0 & 1 - f_0 \\ f_1 f_4 & f_0 f_4 & 0 & f_0 f_1 \end{pmatrix} \quad (3.34)$$

and

$$E_1 = f_0 f_3 f_4, \quad E_2 = f_0 f_1 f_3 f_4, \quad E_3 = f_4 (1 - f_0), \quad E_4 = f_0 f_1 f_3 \quad (3.35)$$

Now using

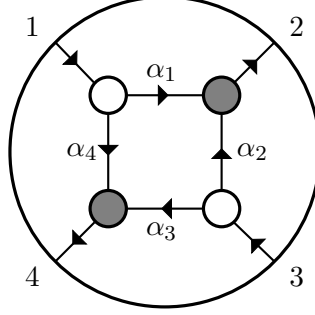
$$f_0 f_1 f_3 f_4 = \frac{\langle 13 \rangle}{\langle 12 \rangle} \quad (3.36)$$

We can put it all together to obtain the form

$$d\Omega = \frac{\langle 12 \rangle}{\langle 13 \rangle} \times \frac{\langle 12 \rangle^2 \langle 13 \rangle}{\langle 23 \rangle \langle 34 \rangle \langle 41 \rangle} \times \frac{1}{\langle 12 \rangle^4} \times \delta^4(P) \delta^8(\mathcal{Q}) = \frac{\delta^8(\mathcal{Q}) \delta^4(P)}{\langle 12 \rangle \langle 23 \rangle \langle 34 \rangle \langle 41 \rangle} \quad (3.37)$$

3.2.2 Using edge-variables

For the remainder of the report we will use instead be using edge-variables in the C -matrices. To demonstrate how this approach works, we look at a diagram with a different orientation,



The C -matrix and its inverse are

$$C = \begin{pmatrix} 1 & \alpha_1 & 0 & \alpha_4 \\ 0 & \alpha_2 & 1 & \alpha_3 \end{pmatrix}, \quad C^\perp = \begin{pmatrix} -\alpha_1 & 1 & -\alpha_2 & 0 \\ -\alpha_4 & 0 & -\alpha_3 & 1 \end{pmatrix} \quad (3.38)$$

The delta-function constraint on C^\perp gives the following equations

$$\delta(C^\perp \cdot \lambda) \rightarrow \begin{cases} -\alpha_1 \lambda_1 + \lambda_2 - \alpha_3 \lambda_3 & = 0 \\ -\alpha_4 \lambda_1 - \alpha_2 \lambda_3 + \lambda_4 & = 0 \end{cases} \quad (3.39)$$

Which after contracting with λ_1 and λ_2 turns into

$$\begin{aligned} \langle 21 \rangle - \alpha_2 \langle 31 \rangle &= 0 \Rightarrow \alpha_2 = \frac{\langle 12 \rangle}{\langle 13 \rangle} \\ \alpha_1 \langle 12 \rangle - \alpha_3 \langle 23 \rangle &= 0 \Rightarrow \alpha_1 = \alpha_2 \frac{\langle 23 \rangle}{\langle 12 \rangle} = \frac{\langle 23 \rangle}{\langle 13 \rangle} \end{aligned} \quad (3.40)$$

Similarly we find

$$\alpha_3 = \frac{\langle 14 \rangle}{\langle 13 \rangle}, \quad \alpha_4 = \frac{\langle 43 \rangle}{\langle 13 \rangle} \quad (3.41)$$

For the other delta function $\delta(C \cdot \tilde{\lambda})$ we get the two equations. The first one is

$$\begin{aligned} 0 &= \tilde{\lambda}_1 + \alpha_2 \tilde{\lambda}_2 + \alpha_4 \tilde{\lambda}_4 = \tilde{\lambda}_1 + \frac{\langle 23 \rangle}{\langle 13 \rangle} \tilde{\lambda}_2 + \frac{\langle 43 \rangle}{\langle 13 \rangle} \tilde{\lambda}_4 \\ \Rightarrow 0 &= \langle 13 \rangle \tilde{\lambda}_1 + \langle 23 \rangle \tilde{\lambda}_2 + \langle 43 \rangle \tilde{\lambda}_4 \end{aligned} \quad (3.42)$$

While the second one is found similarly

$$0 = \langle 21 \rangle \tilde{\lambda}_2 + \langle 31 \rangle \tilde{\lambda}_2 + \langle 41 \rangle \tilde{\lambda}_4 \quad (3.43)$$

We see that the two equations can be obtained from a single momentum conservation equation by contracting with λ_3 and λ_1 respectively. I.e. we have

$$\delta^4(\lambda_1 \tilde{\lambda}_1 + \lambda_2 \tilde{\lambda}_2 + \lambda_3 \tilde{\lambda}_3 + \lambda_4 \tilde{\lambda}_4) \equiv \delta^4(P) \quad (3.44)$$

For the last delta-function we get the exact same thing except for replacing $\tilde{\lambda}_i \rightarrow \tilde{\eta}_i$

$$\delta^8(\lambda_1 \tilde{\eta}_1 + \lambda_2 \tilde{\eta}_2 + \lambda_3 \tilde{\eta}_3 + \lambda_4 \tilde{\eta}_4) \equiv \delta^8(\mathcal{Q}) \quad (3.45)$$

Note that we get an extra factor of $\frac{1}{\langle 13 \rangle^4}$ from re-writing the delta-functions in by projecting along λ_1 and λ_3 . Finally we have

$$\frac{1}{\alpha_1 \alpha_2 \alpha_3 \alpha_4} = \frac{\langle 13 \rangle^4}{\langle 12 \rangle \langle 23 \rangle \langle 34 \rangle \langle 41 \rangle} \quad (3.46)$$

We can now calculate the form

$$d\Omega = \frac{\delta^8(\mathcal{Q}) \delta^4(P)}{\langle 12 \rangle \langle 23 \rangle \langle 34 \rangle \langle 41 \rangle} \quad (3.47)$$

In the next section we will go over examples using these techniques described here at five and six points.

4 Examples of on-shell diagrams at five and six points

In this section we present results for $\mathcal{N} = 4$ sYM at five and six points, which will serve as a springboard to consider forms at $\mathcal{N} \neq 4$.

4.1 Five point

One can build all the physically relevant on-shell diagrams by attaching BCFW bridges to existing diagrams. Here we construct a five point diagram by adding three vertices to a four point graph.

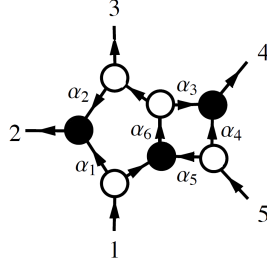


Figure 2. Five point on-shell diagram

The C matrix is

$$C = \begin{pmatrix} 1 & \alpha_1 + \alpha_2\alpha_6 & \alpha_6 & \alpha_3\alpha_6 & 0 \\ 0 & \alpha_5\alpha_6\alpha_2 & \alpha_5\alpha_6 & \alpha_4 + \alpha_3\alpha_5\alpha_6 & 1 \end{pmatrix} \quad (4.1)$$

with the inverse being

$$C^\perp = \begin{pmatrix} -(\alpha_1 + \alpha_2\alpha_6) & 1 & 0 & 0 & -\alpha_5\alpha_6\alpha_2 \\ -\alpha_6 & 0 & 1 & 0 & -\alpha_5\alpha_6 \\ -\alpha_3\alpha_6 & 0 & 0 & 1 & -(\alpha_4 + \alpha_3\alpha_5\alpha_6) \end{pmatrix} \quad (4.2)$$

The amplitude is found through

$$d\Omega = \frac{d\alpha_1}{\alpha_1} \frac{d\alpha_2}{\alpha_2} \frac{d\alpha_3}{\alpha_3} \frac{d\alpha_4}{\alpha_4} \frac{d\alpha_5}{\alpha_5} \frac{d\alpha_6}{\alpha_6} \delta(C \cdot \tilde{\lambda}) \delta(C^\perp \cdot \lambda) \delta(C \cdot \tilde{\eta}) \quad (4.3)$$

Using the delta-function $\delta(C^\perp \cdot \lambda)$ to solve for the α 's we obtain, after contracting with λ_1 , λ_3 , and λ_5 ,

$$\alpha_1 = \frac{\langle 23 \rangle}{\langle 13 \rangle}, \quad \alpha_2 = \frac{\langle 12 \rangle}{\langle 13 \rangle}, \quad \alpha_3 = \frac{\langle 45 \rangle}{\langle 35 \rangle}, \quad \alpha_4 = \frac{\langle 34 \rangle}{\langle 34 \rangle}, \quad \alpha_5 = \frac{\langle 13 \rangle}{\langle 35 \rangle}, \quad \alpha_6 = \frac{\langle 35 \rangle}{\langle 15 \rangle} \quad (4.4)$$

From which we get a Jacobian of $\frac{1}{\langle 15 \rangle^2 \langle 13 \rangle}$. Plugging these α 's back into $\delta(C \cdot \tilde{\lambda})$, we get

$$\begin{aligned} 0 &= \tilde{\lambda}_1 + \tilde{\lambda}_2 \frac{\langle 25 \rangle}{\langle 15 \rangle} + \tilde{\lambda}_3 \frac{\langle 35 \rangle}{\langle 15 \rangle} + \tilde{\lambda}_4 \frac{\langle 45 \rangle}{\langle 15 \rangle} \\ 0 &= \tilde{\lambda}_2 \frac{\langle 12 \rangle}{\langle 15 \rangle} + \tilde{\lambda}_3 \frac{\langle 13 \rangle}{\langle 15 \rangle} + \tilde{\lambda}_4 \frac{\langle 14 \rangle}{\langle 15 \rangle} + \tilde{\lambda}_5 \end{aligned} \quad (4.5)$$

where we have used Schouten identities on the $\tilde{\lambda}_2$ term in the first equation and $\tilde{\lambda}_4$ term in the second equation. We find that

$$\delta(C \cdot \lambda) = \langle 15 \rangle^2 \delta(P) \quad (4.6)$$

Then we plug the α 's into the Grassmann delta function. This will of course give a similar result with the exchange of $\tilde{\lambda} \rightarrow \tilde{\eta}$, although with the Jacobian factor now being $\frac{1}{\langle 15 \rangle^4}$. Finally we calculate

$$\prod_i \frac{1}{\alpha_i} = \frac{\langle 13 \rangle \langle 15 \rangle^2 \langle 35 \rangle^2}{\langle 12 \rangle \langle 23 \rangle \langle 34 \rangle \langle 45 \rangle \langle 51 \rangle} \quad (4.7)$$

From which we are now easily able to get the form

$$d\Omega = \frac{\delta^8(Q) \delta^4(P)}{\langle 12 \rangle \langle 23 \rangle \langle 34 \rangle \langle 45 \rangle \langle 51 \rangle} \quad (4.8)$$

4.2 Six-point NMHV

For the NMHV ($k = 3$) amplitude at six-points we get three different diagrams. In our case we will look at

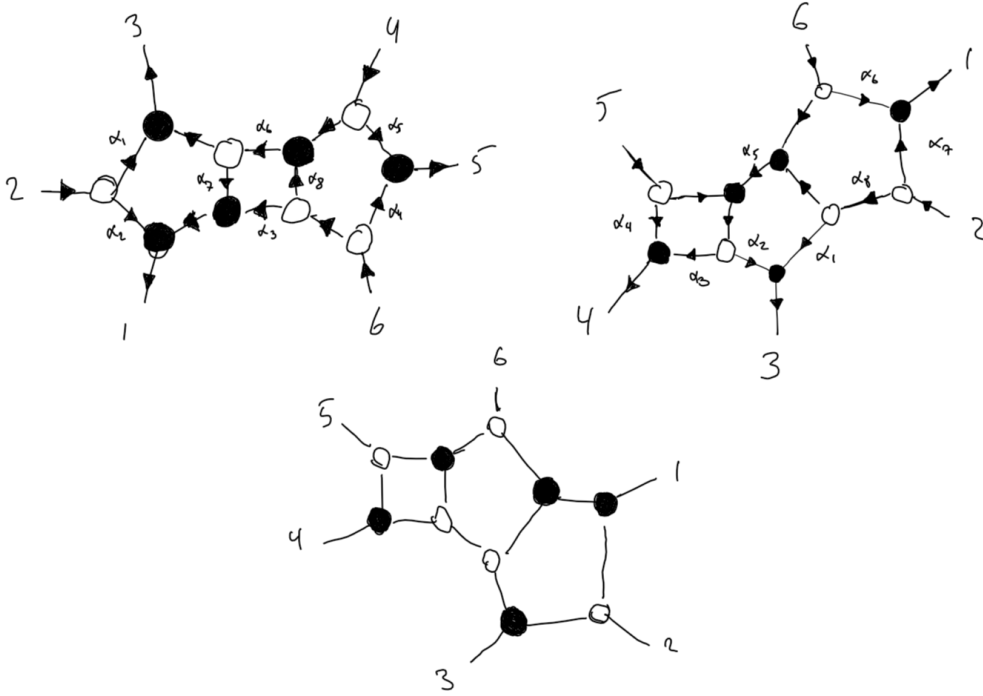


Figure 3. Diagrams contributing to the six point NMHV six point amplitude

We first look at the 4+4 diagram, which has the following C-matrices

$$C = \begin{pmatrix} \alpha_2 & 1 & \alpha_1 & 0 & 0 & 0 \\ \alpha_6 \alpha_7 & 0 & \alpha_6 & 1 & \alpha_5 & 0 \\ \alpha_3 + \alpha_6 \alpha_7 \alpha_8 & 0 & \alpha_6 \alpha_8 & 0 & \alpha_4 & 1 \end{pmatrix}, \quad C^\perp = \begin{pmatrix} 1 - \alpha_2 & 0 & -\alpha_6 \alpha_7 & 0 & -\alpha_3 - \alpha_6 \alpha_7 \alpha_8 \\ 0 & -\alpha_1 & 1 & -\alpha_6 & 0 & -\alpha_6 \alpha_8 \\ 0 & 0 & 0 & -\alpha_5 & 1 & -\alpha_4 \end{pmatrix} \quad (4.9)$$

We then use the following combination of equation from the $C \cdot \tilde{\lambda}$ and $C_{\perp} \cdot \lambda$ delta functions

$$\begin{aligned}
0 &= -\langle 23 \rangle + \alpha_4 \langle 24 \rangle, & 0 &= -(\alpha_5 \langle 24 \rangle) + \langle 34 \rangle \\
0 &= [61] - \alpha_2 [15], & 0 &= [65] + \alpha_1 [15] \\
0 &= -[12] - \alpha_5 [13] - \alpha_6 \alpha_7 [15], & 0 &= \alpha_6 [15] + [25] + \alpha_5 [35] \\
0 &= -(\alpha_4 [13]) - [14] - (\alpha_3 + \alpha_6 \alpha_7 \alpha_8) [15], & 0 &= \alpha_6 \alpha_8 [15] + \alpha_4 [35] + [45]
\end{aligned} \tag{4.10}$$

to obtain

$$\begin{aligned}
\alpha_1 &= -\frac{[65]}{[15]}, \quad \alpha_2 = \frac{[61]}{[15]}, \quad \alpha_3 = \frac{s_{234}}{\langle 4|Q_{234}|5 \rangle}, \quad \alpha_4 = \frac{\langle 23 \rangle}{\langle 24 \rangle}, \quad \alpha_5 = \frac{\langle 34 \rangle}{\langle 24 \rangle}, \\
\alpha_6 &= \frac{\langle 4|Q_{234}|5 \rangle}{\langle 24 \rangle [15]}, \quad \alpha_7 = -\frac{\langle 4|Q_{234}|1 \rangle}{\langle 4|Q_{234}|5 \rangle}, \quad \alpha_8 = -\frac{\langle 2|Q_{234}|5 \rangle}{\langle 4|Q_{234}|5 \rangle}.
\end{aligned}$$

where $Q_{ijk} = p_i + p_j + p_k$. For the other delta functions we get

$$\begin{aligned}
0 &= \tilde{\eta}_1 - \frac{[65]}{[15]} \tilde{\eta}_2 + \frac{[61]}{[15]} \tilde{\eta}_6 \\
0 &= \frac{\langle 4|Q_{234}|5 \rangle}{\langle 24 \rangle [15]} \tilde{\eta}_1 + \tilde{\eta}_2 + \frac{\langle 34 \rangle}{\langle 24 \rangle} \tilde{\eta}_4 - \frac{\langle 3|Q_{234}|1 \rangle}{\langle 24 \rangle [15]} \tilde{\eta}_6 \\
0 &= -\frac{\langle 2|Q_{234}|5 \rangle}{\langle 24 \rangle [15]} \tilde{\eta}_2 + \frac{\langle 23 \rangle}{\langle 24 \rangle} \tilde{\eta}_4 + \tilde{\eta}_5 + \frac{s_{234} \langle 24 \rangle [15] + \langle 2|Q_{234}|5 \rangle \langle 4|Q_{234}|1 \rangle}{\langle 4|Q_{234}|5 \rangle} \tilde{\eta}_5
\end{aligned} \tag{4.11}$$

The Jacobian from the delta functions is

$$J = \frac{1}{[15]^3 \langle 24 \rangle^3 \langle 4|Q_{234}|5 \rangle^2} \tag{4.12}$$

and we get the form

$$d\Omega_1 = \frac{\delta(\sum P) \delta(\tilde{\eta}_5 [16] + \tilde{\eta}_6 [15] + \tilde{\eta}_1 [56])}{s_{234} \langle 23 \rangle \langle 34 \rangle [61] [56] \langle 2|Q_{234}|5 \rangle \langle 4|Q_{234}|1 \rangle} \tag{4.13}$$

Looking at the 5+3 diagram we get the following C-matrix

$$\begin{aligned}
C &= \begin{pmatrix} \alpha_7 & 1 & \alpha_8(\alpha_1 + \alpha_2 \alpha_5) & \alpha_3 \alpha_5 \alpha_8 & 0 & 0 \\ 0 & 0 & \alpha_2 & \alpha_3 + \alpha_4 & 1 & 0 \\ \alpha_6 & 0 & \alpha_2 \alpha_5 & \alpha_3 \alpha_5 & 0 & 1 \end{pmatrix} \\
C_{\perp} &= \begin{pmatrix} 1 & -\alpha_7 & 0 & 0 & 0 & -\alpha_6 \\ 0 & -\alpha_8(\alpha_1 + \alpha_2 \alpha_5) & 1 & 0 & -\alpha_2 & -\alpha_2 \alpha_5 \\ 0 & -\alpha_3 \alpha_5 \alpha_8 & 0 & 1 & -\alpha_3 - \alpha_4 & -\alpha_3 \alpha_5 \end{pmatrix}
\end{aligned} \tag{4.14}$$

From the delta functions $\delta(C \cdot \tilde{\lambda})$ and $\delta(C_{\perp} \cdot \lambda)$, we use the following equations

$$\begin{aligned}
0 &= \langle 26 \rangle - (\alpha_3 + \alpha_4) \langle 36 \rangle - \alpha_3 \alpha_5 \langle 46 \rangle, & 0 &= -\langle 45 \rangle + \alpha_7 \langle 46 \rangle, \\
0 &= -\alpha_6 \langle 46 \rangle + \langle 56 \rangle, & 0 &= -(\alpha_3 + \alpha_4) [12] - [13], \\
0 &= \alpha_2 [12] - [23], & 0 &= \alpha_2 \alpha_5 [12] - [24] - \alpha_6 [25], \\
0 &= -\alpha_3 \alpha_5 \alpha_8 [12] - \alpha_7 [15] - [16], & 0 &= (\alpha_1 + \alpha_2 \alpha_5) \alpha_8 [12] - \alpha_7 [25] - [26],
\end{aligned} \tag{4.15}$$

to obtain solutions for the edge-variables

$$\begin{aligned}\alpha_1 &= \frac{s_{612}}{\langle 6|Q_{612}|3\rangle}, & \alpha_2 &= \frac{[45]}{[34]}, & \alpha_3 &= \frac{[45]\langle 2|Q_{612}|3\rangle}{[34]\langle 2|Q_{612}|4\rangle}, & \alpha_4 &= \frac{\langle 2|Q_{612}|5\rangle}{\langle 2|Q_{612}|4\rangle}, \\ \alpha_5 &= \frac{\langle 2|Q_{612}|4\rangle}{\langle 62\rangle[45]}, & \alpha_6 &= \frac{\langle 12\rangle}{\langle 62\rangle}, & \alpha_7 &= \frac{\langle 61\rangle}{\langle 62\rangle}, & \alpha_8 &= \frac{\langle 6|Q_{612}|3\rangle}{\langle 2|Q_{612}|3\rangle}.\end{aligned}\tag{4.16}$$

Here the Jacobian from the delta functions is

$$J = \frac{1}{[34]^3 \langle 62\rangle^3 \langle 2|Q_{612}|4\rangle \langle 6|Q_{612}|3\rangle}\tag{4.17}$$

and we get the form

$$d\Omega_2 = \frac{\delta(\sum P)\delta(\tilde{\eta}_3[45] + \tilde{\eta}_4[35] + \tilde{\eta}_5[34])}{s_{612} \langle 12\rangle \langle 16\rangle [34][35] \langle 6|Q_{612}|3\rangle \langle 2|Q_{612}|5\rangle}\tag{4.18}$$

The final diagram can be found by permuting by 2 and exchanging square and angle brackets:

$$d\Omega_3 = \frac{\delta(\sum P)\delta(\tilde{\eta}_1[23] + \tilde{\eta}_2[13] + \tilde{\eta}_3[12])}{s_{456} \langle 45\rangle \langle 56\rangle [23][12] \langle 4|Q_{456}|1\rangle \langle 6|Q_{456}|3\rangle}\tag{4.19}$$

In total we have

$$\begin{aligned}& d\Omega_1 + d\Omega_2 + d\Omega_3 \\ &= \frac{\delta(\sum P)\delta(\tilde{\eta}_5[16] + \tilde{\eta}_6[15] + \tilde{\eta}_1[56])}{s_{234} \langle 23\rangle \langle 34\rangle [61][56] \langle 2|Q_{234}|5\rangle \langle 4|Q_{234}|1\rangle} + \frac{\delta(\sum P)\delta(\tilde{\eta}_3[45] + \tilde{\eta}_4[35] + \tilde{\eta}_5[34])}{s_{612} \langle 12\rangle \langle 16\rangle [34][35] \langle 6|Q_{612}|3\rangle \langle 2|Q_{612}|5\rangle} \\ &+ \frac{\delta(\sum P)\delta(\tilde{\eta}_1[23] + \tilde{\eta}_2[13] + \tilde{\eta}_3[12])}{s_{456} \langle 45\rangle \langle 56\rangle [23][12] \langle 4|Q_{456}|1\rangle \langle 6|Q_{456}|3\rangle}\end{aligned}\tag{4.20}$$

Then using the fact that

$$\begin{aligned}\mathcal{A}^{(0),\text{MHV}} R_{j,j+3,j+5} &= \\ &= \frac{\delta^{(8)}(\sum \lambda_i \eta_i^A)}{\langle j(j+1)\rangle \langle (j+1)(j+2)\rangle [(j+3)(j+4)] [(j+4)(j+5)]} \\ &\times \frac{\delta^{(4)}(\eta_{j+3}^A [(j+4)(j+5)] + \eta_{j+4}^A [(j+5)(j+3)] + \eta_{j+5}^A [(j+3)(j+4)])}{\langle j|K_{j+1,j+2}|(j+3)\rangle \langle (j+2)|K_{j+3,j+4}|(j+5)\rangle s_{j,j+1,j+2}}.\end{aligned}\tag{4.21}$$

We find that the full NMHV amplitude can be written as

$$A_6^{\text{NMHV}} = A_6^{\text{MHV}} (R_{251} + R_{413} + R_{635})\tag{4.22}$$

Having now showed the general procedure to calculate forms from the on-shell diagrams, we will show how to extend this approach to amplitudes with $\mathcal{N} \neq 4$ super-symmetries.

5 Calculating $\mathcal{N} < 4$ amplitudes

5.1 The measure

Since going to $\mathcal{N} < 4$ means that the graphs have to be oriented, one has to consider all internal orientations for specific external helicity configurations. Further, for diagrams containing closed internal loops, one has to add an extra factor, \mathcal{J} , in the measure,

$$d\Omega = \frac{d\alpha_1}{\alpha_1} \frac{d\alpha_2}{\alpha_2} \dots \frac{d\alpha_m}{\alpha_m} \mathcal{J}^{\mathcal{N}-4} \delta(C \cdot Z), \quad (5.1)$$

where this Jacobian is given by

$$\mathcal{J} = 1 + \sum_i f_i + \sum_{\substack{\text{disjoint} \\ \text{pairs } i,j}} f_i f_j + \sum_{\substack{\text{disjoint} \\ \text{pairs } i,j,k}} f_i f_j f_k + \dots \quad (5.2)$$

with f_i denoting the face of a closed cycle, and the sums are over disjoint collections of these closed cycles. One also has to note that each face is defined as *clockwise-oriented product of edge-variables*, meaning that a counterclockwise cycle would produce $\frac{1}{f}$. In the following sections we will specifically consider $\mathcal{N} = 0$ for which one also has to take $\delta(C^\perp \cdot \lambda) \delta(C \cdot \tilde{\lambda})$.

5.2 Four-point $\mathcal{N} = 0$ with internal loop

The simplest example is at four points where we have two diagrams after fixing the external helicities

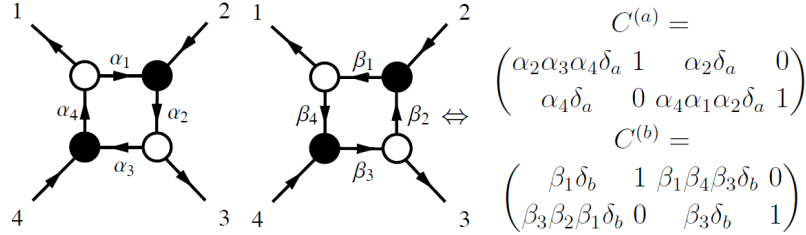


Figure 4. All diagrams contributing to the specified helicity configuration at four points

where the δ' s are defined by

$$\delta_a = \frac{1}{1 - \prod_{i=1}^4 \alpha_i}, \quad \delta_b = \frac{1}{1 - \prod_{i=1}^4 \beta_i} \quad (5.3)$$

Solving the C_\perp delta-function, we get the following equations after contracting with λ_2 and λ_4

$$\begin{aligned} 0 &= \langle 12 \rangle + \frac{\alpha_4 \langle 24 \rangle}{1 - \alpha_1 \alpha_2 \alpha_3 \alpha_4}, & 0 &= \langle 14 \rangle - \frac{\alpha_2 \alpha_3 \alpha_4 \langle 24 \rangle}{1 - \alpha_1 \alpha_2 \alpha_3 \alpha_4}, \\ 0 &= -\langle 23 \rangle + \frac{\alpha_1 \alpha_2 \alpha_4 \langle 24 \rangle}{1 - \alpha_1 \alpha_2 \alpha_3 \alpha_4}, & 0 &= \langle 34 \rangle - \frac{\alpha_2 \langle 24 \rangle}{1 - \alpha_1 \alpha_2 \alpha_3 \alpha_4} \end{aligned} \quad (5.4)$$

from which we obtain

$$\begin{aligned}\alpha_1 &= -\frac{\langle 23 \rangle}{\langle 13 \rangle}, & \alpha_2 &= \frac{\langle 13 \rangle}{\langle 12 \rangle}, \\ \alpha_3 &= -\frac{\langle 14 \rangle}{\langle 13 \rangle}, & \alpha_4 &= -\frac{\langle 13 \rangle}{\langle 34 \rangle},\end{aligned}\tag{5.5}$$

along with a Jacobian factor from rewriting the delta functions of $\frac{\langle 24 \rangle^2}{\langle 12 \rangle^2 \langle 34 \rangle^2}$. We further find an expression for δ_a

$$\delta_a = \frac{\langle 12 \rangle \langle 34 \rangle}{\langle 13 \rangle \langle 24 \rangle}\tag{5.6}$$

Taking these solutions and inserting into the other delta functions, and multiplying by $\tilde{\lambda}_1$ and $\tilde{\lambda}_3$ we get

$$\begin{aligned}0 &= [12] + \frac{\langle 34 \rangle [13]}{\langle 24 \rangle}, & 0 &= [23] + \frac{\langle 14 \rangle [13]}{\langle 24 \rangle} \\ 0 &= [14] + \frac{\langle 23 \rangle [13]}{\langle 24 \rangle}, & 0 &= [34] + \frac{\langle 12 \rangle [13]}{\langle 24 \rangle}\end{aligned}\tag{5.7}$$

which we can combine into $\delta^4(P) \langle 24 \rangle^2$. Finally the Jacobian is

$$\mathcal{J}_a = 1 - \alpha_1 \alpha_2 \alpha_3 \alpha_4 = \delta_a^{-1} = \frac{\langle 13 \rangle \langle 24 \rangle}{\langle 12 \rangle \langle 34 \rangle}\tag{5.8}$$

The procedure is the same for the other diagram and here we just summarize the results

$$\begin{aligned}\beta_1 &= \frac{\langle 13 \rangle}{\langle 23 \rangle}, & \beta_2 &= \frac{\langle 21 \rangle}{\langle 13 \rangle}, \\ \beta_3 &= \frac{\langle 13 \rangle}{\langle 14 \rangle}, & \beta_4 &= \frac{\langle 34 \rangle}{\langle 13 \rangle},\end{aligned}\tag{5.9}$$

$$\mathcal{J}_b = 1 - \beta_1 \beta_2 \beta_3 \beta_4 = \delta_b^{-1} = \frac{\langle 13 \rangle \langle 24 \rangle}{\langle 14 \rangle \langle 23 \rangle}\tag{5.10}$$

Combining all these factors with $\prod_i \alpha_i = \frac{\langle 41 \rangle \langle 23 \rangle}{\langle 12 \rangle \langle 34 \rangle}$ and $\prod_i \beta_i = \frac{\langle 12 \rangle \langle 34 \rangle}{\langle 23 \rangle \langle 41 \rangle}$, as well as using taking the Jacobians to the -4 'th power, we can combine them in the form

$$d\Omega = \frac{\langle 24 \rangle^4}{\langle 12 \rangle \langle 23 \rangle \langle 34 \rangle \langle 41 \rangle} \left(\left[\frac{\langle 13 \rangle \langle 24 \rangle}{\langle 12 \rangle \langle 34 \rangle} \right]^{-4} + \left[\frac{\langle 13 \rangle \langle 24 \rangle}{\langle 14 \rangle \langle 23 \rangle} \right]^{-4} \right) \delta(P)\tag{5.11}$$

5.3 Five-point $\mathcal{N} = 0$, no internal cycle

For five and six points we will look at two different types of diagrams. First we analyze one without an internal cycle, i.e. has $\mathcal{J} = 1$. As will be evident, this produces the standard Yang-Mills amplitude. We then follow this by evaluating diagrams with internal cycles, which can be used to get forms for $\mathcal{N} \neq 4$. We will once again look at the following diagram

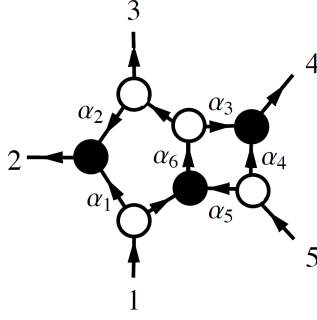


Figure 5. Five point on-shell diagram

We already solved this in section 4, here we obtained the following edge-variables after contracting with λ_1 , λ_3 , and λ_5

$$\alpha_1 = \frac{\langle 23 \rangle}{\langle 13 \rangle}, \quad \alpha_2 = \frac{\langle 12 \rangle}{\langle 13 \rangle}, \quad \alpha_3 = \frac{\langle 45 \rangle}{\langle 35 \rangle}, \quad \alpha_4 = \frac{\langle 34 \rangle}{\langle 34 \rangle}, \quad \alpha_5 = \frac{\langle 13 \rangle}{\langle 35 \rangle}, \quad \alpha_6 = \frac{\langle 35 \rangle}{\langle 15 \rangle} \quad (5.12)$$

and a Jacobian from solving the delta functions of $\frac{\langle 15 \rangle^2}{\langle 35 \rangle^2 \langle 13 \rangle}$. For this diagram we have two negative helicity particles 1 and 5 which is seen from the incoming arrows at those points. The orientation of these external legs do not yield an internal orientation with a closed cycle, and so this is the only diagram we have to take into account and there is no extra Jacobian factor. Using $\prod_i \alpha_i = \frac{\langle 12 \rangle \langle 23 \rangle \langle 34 \rangle \langle 45 \rangle}{\langle 13 \rangle \langle 15 \rangle \langle 35 \rangle^2}$ The form then yields the amplitude

$$\begin{aligned} d\Omega_5(1^-, 2^+, 3^+, 4^+, 5^-) &= \frac{\langle 15 \rangle^2}{\langle 35 \rangle^2 \langle 13 \rangle} \frac{\delta(P)}{\prod_i \alpha_i} \\ &= \frac{\langle 15 \rangle^4}{\langle 12 \rangle \langle 23 \rangle \langle 34 \rangle \langle 45 \rangle \langle 51 \rangle} \delta(P) \end{aligned} \quad (5.13)$$

5.4 Five point with internal cycles

We will now consider a diagram containing internal cycles. For the fixed helicity configuration of $(1^+, 2^-, 3^+, 4^+, 5^-)$ the diagrams below contribute

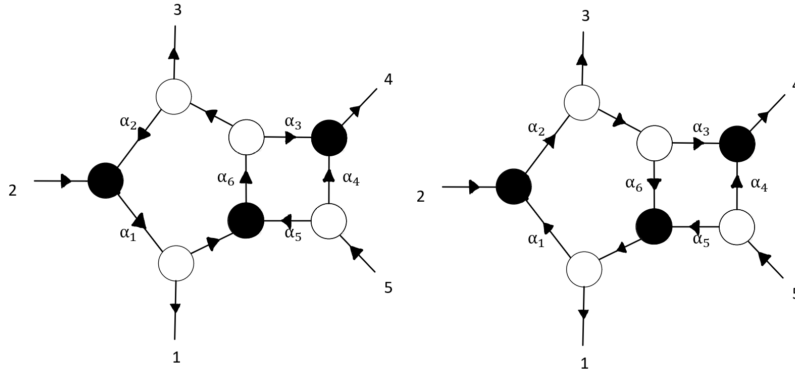


Figure 6. All diagrams for the specified five point helicity configuration

Denoting the left diagram by "a" and the right one by "b", the C -matrices are

$$C_a = \begin{pmatrix} \alpha_1 \delta_a & 1 & \alpha_1 \alpha_6 \delta_a & \alpha_1 \alpha_3 \alpha_6 \delta_a & 0 \\ \alpha_1 \alpha_2 \alpha_5 \alpha_6 \delta_a & 0 & \alpha_5 \alpha_6 \delta_a & \alpha_3 \alpha_5 \alpha_6 \delta_a + \alpha_4 & 1 \end{pmatrix}, \quad C_a^\perp = \begin{pmatrix} 1 & -\alpha_1 \delta_a & 0 & 0 & -\alpha_1 \alpha_2 \alpha_5 \alpha_6 \delta_a \\ 0 & -\alpha_1 \alpha_6 \delta_a & 1 & 0 & -\alpha_5 \alpha_6 \delta_a \\ 0 & -\alpha_1 \alpha_3 \alpha_6 \delta_a & 0 & 1 & -\alpha_3 \alpha_5 \alpha_6 \delta_a - \alpha_4 \end{pmatrix}$$

$$C_b = \begin{pmatrix} \beta_2 \beta_6 \delta_b & 1 & \beta_2 \delta_b & \beta_2 \beta_3 \delta_b & 0 \\ \beta_5 \delta_b & 0 & \beta_1 \beta_2 \beta_5 \delta_b & \beta_1 \beta_2 \beta_3 \beta_5 \delta_b + \beta_4 & 1 \end{pmatrix}, \quad C_b^\perp = \begin{pmatrix} 1 & -\beta_2 \beta_6 \delta_b & 0 & 0 & -\beta_5 \delta_b \\ 0 & -\beta_2 \delta_b & 1 & 0 & -\beta_1 \beta_2 \beta_5 \delta_b \\ 0 & -\beta_2 \beta_3 \delta_b & 0 & 1 & -\beta_1 \beta_2 \beta_3 \beta_5 \delta_b - \beta_4 \end{pmatrix} \quad (5.14)$$

Solving the delta-function constraints we are led to the following solutions for the edge variables

$$\alpha_1 = \frac{\langle 13 \rangle}{\langle 23 \rangle}, \quad \alpha_2 = -\frac{\langle 12 \rangle}{\langle 13 \rangle}, \quad \alpha_3 = \frac{\langle 45 \rangle}{\langle 35 \rangle}, \quad \alpha_4 = \frac{\langle 34 \rangle}{\langle 35 \rangle}, \quad \alpha_5 = \frac{\langle 13 \rangle}{\langle 35 \rangle}, \quad \alpha_6 = \frac{\langle 35 \rangle}{\langle 15 \rangle}$$

$$\beta_1 = -\frac{\langle 23 \rangle}{\langle 13 \rangle}, \quad \beta_2 = -\frac{\langle 13 \rangle}{\langle 12 \rangle}, \quad \beta_3 = \frac{\langle 45 \rangle}{\langle 35 \rangle}, \quad \beta_4 = \frac{\langle 34 \rangle}{\langle 35 \rangle}, \quad \beta_5 = -\frac{\langle 13 \rangle}{\langle 35 \rangle}, \quad \beta_6 = \frac{\langle 15 \rangle}{\langle 35 \rangle} \quad (5.15)$$

along with a Jacobian from solving the delta functions of $\frac{\langle 13 \rangle \langle 25 \rangle^4}{\langle 15 \rangle^2 \langle 23 \rangle^2 \langle 35 \rangle^2}$ and $\frac{\langle 13 \rangle \langle 25 \rangle^4}{\langle 12 \rangle^2 \langle 35 \rangle^2}$ respectively. The Jacobians from the internal loops are

$$\mathcal{J}_a = \delta_a^{-1} = \frac{\langle 13 \rangle \langle 25 \rangle}{\langle 15 \rangle \langle 23 \rangle}, \quad \mathcal{J}_b = \delta_b^{-1} = \frac{\langle 13 \rangle \langle 25 \rangle}{\langle 12 \rangle \langle 35 \rangle} \quad (5.16)$$

One can note that these can be rewritten using Schouten,

$$\mathcal{J}_a = 1 + \frac{\langle 12 \rangle \langle 35 \rangle}{\langle 15 \rangle \langle 23 \rangle} \equiv 1 + f^{-1}, \quad \mathcal{J}_b = 1 + \frac{\langle 15 \rangle \langle 23 \rangle}{\langle 12 \rangle \langle 35 \rangle} \equiv 1 + f \quad (5.17)$$

and since, as we will see shortly, the forms produced by the individual diagrams only differ by this Jacobian, one does not have to go through the calculation of both diagrams, but can instead infer, the Jacobian by rewriting it in this form. Similarly we will also find that changing the direction of an arrow, just flips the expression for the edge $\alpha_k \rightarrow \frac{1}{\alpha_k}$, from which the Jacobian of the reverse cycle diagram can be found.

Using this, the $\mathcal{N} = 0$ form for the cut is found by adding the diagrams

$$\begin{aligned} d\Omega &= \left(\frac{\langle 13 \rangle \langle 25 \rangle^4}{\langle 15 \rangle^2 \langle 23 \rangle^2 \langle 35 \rangle^2} J_a^{-4} \prod_{i=1}^5 \frac{1}{\alpha_i} + \frac{\langle 13 \rangle \langle 25 \rangle^4}{\langle 12 \rangle^2 \langle 35 \rangle^2} J_b^{-4} \prod_{i=1}^5 \frac{1}{\beta_i} \right) \delta(P) \\ &= \frac{\langle 25 \rangle^4}{\langle 12 \rangle \langle 23 \rangle \langle 34 \rangle \langle 45 \rangle \langle 51 \rangle} \delta(P) (J_a^{-4} + J_b^{-4}) \\ &= \frac{\langle 15 \rangle^4 \langle 23 \rangle^4 + \langle 12 \rangle^4 \langle 35 \rangle^4}{\langle 13 \rangle^4 \langle 12 \rangle \langle 23 \rangle \langle 34 \rangle \langle 45 \rangle \langle 51 \rangle} \delta(P) \end{aligned} \quad (5.18)$$

As described, the only difference between the two diagrams is the Jacobian. To complete the picture we will consider one further example, by changing the external helicity configuration to $(1^-, 2^+, 3^+, 4^-, 5^+)$. Here the diagrams below contribute

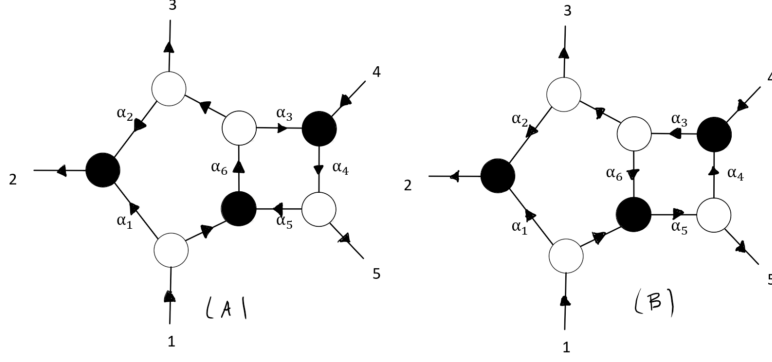


Figure 7. All diagrams for the specified five point helicity configuration

We will just consider the "A" diagram and then apply the above method to get the Jacobian from the "B" orientation. We obtain

$$\begin{aligned}
 C_A &= \begin{pmatrix} 1 & \alpha_2 \alpha_6 \delta_a + \alpha_1 & \alpha_6 \delta_a & 0 & \alpha_3 \alpha_4 \alpha_6 \delta_a \\ 0 & \alpha_2 \alpha_4 \alpha_5 \alpha_6 \delta_a & \alpha_4 \alpha_5 \alpha_6 \delta_a & 1 & \alpha_4 \delta_a \end{pmatrix} \\
 C_A^\perp &= \begin{pmatrix} -\alpha_2 \alpha_6 \delta - \alpha_1 & 1 & 0 & -\alpha_2 \alpha_4 \alpha_5 \alpha_6 \delta & 0 \\ -\alpha_6 \delta & 0 & 1 & -\alpha_4 \alpha_5 \alpha_6 \delta & 0 \\ -\alpha_3 \alpha_4 \alpha_6 \delta & 0 & 0 & -\alpha_4 \delta & 1 \end{pmatrix}
 \end{aligned} \tag{5.19}$$

$$\alpha_1 = \frac{\langle 23 \rangle}{\langle 13 \rangle}, \quad \alpha_2 = \frac{\langle 12 \rangle}{\langle 13 \rangle}, \quad \alpha_3 = -\frac{\langle 45 \rangle}{\langle 35 \rangle}, \quad \alpha_4 = \frac{\langle 35 \rangle}{\langle 34 \rangle}, \quad \alpha_5 = \frac{\langle 13 \rangle}{\langle 35 \rangle}, \quad \alpha_6 = \frac{\langle 35 \rangle}{\langle 15 \rangle} \tag{5.20}$$

with

$$J_a = \frac{\langle 14 \rangle \langle 35 \rangle}{\langle 15 \rangle \langle 34 \rangle}, \quad J_b = \frac{\langle 14 \rangle \langle 35 \rangle}{\langle 13 \rangle \langle 45 \rangle} \tag{5.21}$$

and the $\mathcal{N} = 0$ form for the cut is found to be

$$d\Omega = \frac{\langle 14 \rangle^4}{\langle 12 \rangle \langle 23 \rangle \langle 34 \rangle \langle 45 \rangle \langle 51 \rangle} \delta(P) \left(\left[\frac{\langle 14 \rangle \langle 35 \rangle}{\langle 15 \rangle \langle 34 \rangle} \right]^{-4} + \left[\frac{\langle 14 \rangle \langle 35 \rangle}{\langle 13 \rangle \langle 45 \rangle} \right]^{-4} \right) \tag{5.22}$$

5.5 Six-point $\mathcal{N} = 0$

To illustrate what the form of the bare² diagram should look like we start by treating a diagram without an internal cycle. We take the same diagram as we did in section 4.

²By bare we mean the form without the internal cycle Jacobian

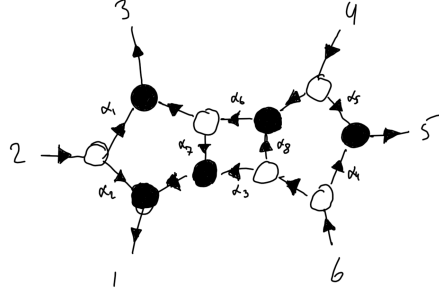


Figure 8. 4+4 NMHV six point diagram

where we obtained

$$\alpha_1 = -\frac{[65]}{[15]}, \quad \alpha_2 = \frac{[61]}{[15]}, \quad \alpha_3 = \frac{s_{234}}{\langle 4|Q_{234}|5\rangle}, \quad \alpha_4 = \frac{\langle 23\rangle}{\langle 24\rangle}, \quad \alpha_5 = \frac{\langle 34\rangle}{\langle 24\rangle},$$

$$\alpha_6 = \frac{\langle 4|Q_{234}|5\rangle}{\langle 24\rangle[15]}, \quad \alpha_7 = -\frac{\langle 4|Q_{234}|1\rangle}{\langle 4|Q_{234}|5\rangle}, \quad \alpha_8 = -\frac{\langle 2|Q_{234}|5\rangle}{\langle 4|Q_{234}|5\rangle}.$$

The Jacobian from solving the delta functions is $J = \frac{[15]\langle 24\rangle}{\langle 4|Q_{234}|5\rangle^2}$, such that the form is given by

$$d\Omega_{4+4} = \frac{\langle 24\rangle^4 [15]^4}{s_{234} \langle 23\rangle \langle 34\rangle \langle 2|Q_{234}|5\rangle \langle 4|Q_{234}|1\rangle [61][56]} \quad (5.23)$$

One would expect the bare form to look something like this in the next examples. We proceed by looking at diagrams with internal cycles, after which we analyze the singularity structure.

5.6 Six point NMHV with internal cycles

We now consider a six point diagram with an internal cycle. Fixing the helicity configuration to $(1^+, 2^-, 3^+, 4^-, 5^+, 6^-)$ and considering the 5+3 diagrams yields

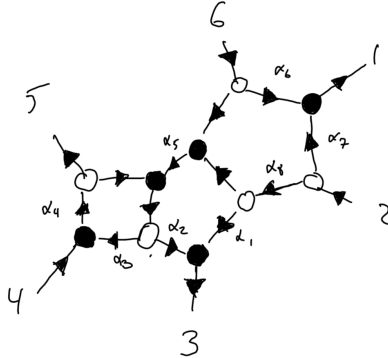


Figure 9. 5+3 six-point NMHV diagram with internal cycle. To calculate the form of the cut, the same diagram with the cycle reversed also contributes.

Where another diagram with the internal cycle is reversed also contributes to the form of the cut. The edge-variables are found to be

$$\begin{aligned}\alpha_1 &= \frac{s_{612}}{\langle 6|Q_{612}|3\rangle}, & \alpha_2 &= \frac{[45]}{[34]}, & \alpha_3 &= \frac{[45]\langle 2|Q_{612}|3\rangle}{[34]\langle 2|Q_{612}|4\rangle}, & \alpha_4 &= -\frac{\langle 2|Q_{612}|4\rangle}{\langle 2|Q_{612}|5\rangle}, \\ \alpha_5 &= \frac{\langle 2|Q_{612}|4\rangle}{\langle 62\rangle[45]}, & \alpha_6 &= \frac{\langle 12\rangle}{\langle 62\rangle}, & \alpha_7 &= \frac{\langle 61\rangle}{\langle 62\rangle}, & \alpha_8 &= -\frac{\langle 6|Q_{612}|3\rangle}{\langle 2|Q_{612}|3\rangle}.\end{aligned}\quad (5.24)$$

The Jacobian from solving the delta functions is $\frac{\langle 26\rangle[35]^4\langle 2|Q_{612}|4\rangle}{[34]^3\langle 2|Q_{612}|5\rangle^2\langle 2|Q_{612}|3\rangle}$ while the internal cycle Jacobian is

$$J_a = \frac{\langle 2|Q_{612}|4\rangle[35]}{\langle 2|Q_{612}|5\rangle[34]} \quad (5.25)$$

Using the approach described at five-point we can infer the Jacobian of the diagram with opposite cycle to be

$$J_b = \frac{\langle 2|Q_{612}|4\rangle[35]}{\langle 2|Q_{612}|3\rangle[45]} \quad (5.26)$$

The form is then

$$d\Omega = \frac{\langle 26\rangle^4[24]^4\delta(P)}{s_{612}\langle 12\rangle\langle 16\rangle[34][45]\langle 2|Q_{612}|5\rangle\langle 6|Q_{612}|3\rangle} \left[\left(\frac{\langle 2|Q_{612}|4\rangle[35]}{\langle 2|Q_{612}|5\rangle[34]} \right)^{-4} + \left(\frac{\langle 2|Q_{612}|4\rangle[35]}{\langle 2|Q_{612}|3\rangle[45]} \right)^{-4} \right] \quad (5.27)$$

Let us further examine the six-point NMHV case by looking at an example of a 4+4 diagram. It is not possible to orient the graph with a closed cycle for the external helicity configuration of $(1^+, 2^-, 3^+, 4^-, 5^+, 6^-)$, so instead we consider the following two diagrams.

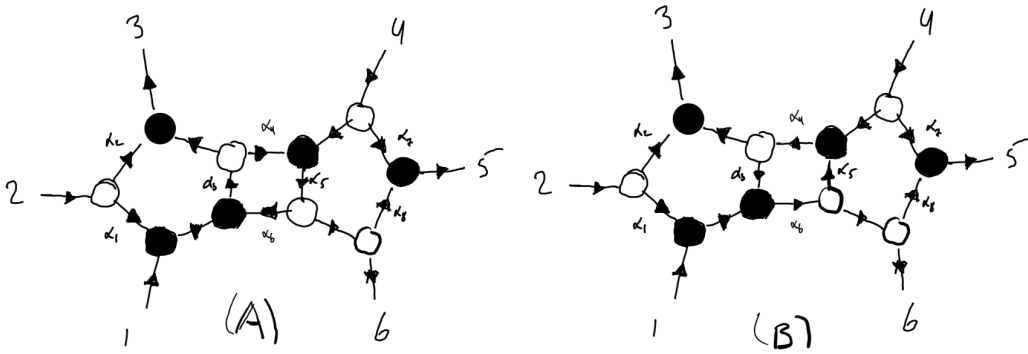


Figure 10. All six point NMHV diagrams for the specific helicity configuration

They are the only ones that arise when fixing the internal states as shown. Here we explicitly

show the C_A -matrices

$$\begin{aligned}
C_A &= \begin{pmatrix} 1 & 0 & \alpha_3 \delta_a & 0 & \alpha_3 \alpha_4 \alpha_5 \alpha_8 \delta_a & \alpha_3 \alpha_4 \alpha_5 \delta_a \\ 0 & 1 & \alpha_1 \alpha_3 \delta_a + \alpha_2 & 0 & \alpha_1 \alpha_3 \alpha_4 \alpha_5 \alpha_8 \delta_a & \alpha_1 \alpha_3 \alpha_4 \alpha_5 \delta_a \\ 0 & 0 & \alpha_3 \alpha_5 \alpha_6 \delta_a & 1 & \alpha_5 \alpha_8 \delta_a + \alpha_7 & \alpha_5 \delta_a \end{pmatrix} \\
C_A^\perp &= \begin{pmatrix} -\alpha_3 \delta_a & -\alpha_1 \alpha_3 \delta_a - \alpha_2 & 1 & -\alpha_3 \alpha_5 \alpha_6 \delta_a & 0 & 0 \\ -\alpha_3 \alpha_4 \alpha_5 \alpha_8 \delta_a & -\alpha_1 \alpha_3 \alpha_4 \alpha_5 \alpha_8 \delta_a & 0 & -\alpha_5 \alpha_8 \delta_a - \alpha_7 & 1 & 0 \\ -\alpha_3 \alpha_4 \alpha_5 \delta_a & -\alpha_1 \alpha_3 \alpha_4 \alpha_5 \delta_a & 0 & -\alpha_5 \delta_a & 0 & 1 \end{pmatrix}
\end{aligned} \tag{5.28}$$

The edge-variables for diagram A are found to be

$$\begin{aligned}
\alpha_1 &= \frac{[23]}{[13]}, \quad \alpha_2 = -\frac{[12]}{[13]}, \quad \alpha_3 = -\frac{\langle 6|Q_{456}|1\rangle}{\langle 6|Q_{456}|3\rangle}, \quad \alpha_4 = \frac{\langle 46\rangle[13]}{\langle 6|Q_{456}|1\rangle}, \\
\alpha_5 &= \frac{\langle 6|Q_{456}|1\rangle}{\langle 4|Q_{456}|1\rangle}, \quad \alpha_6 = \frac{s_{456}}{\langle 6|Q_{456}|1\rangle}, \quad \alpha_7 = \frac{\langle 56\rangle}{\langle 46\rangle}, \quad \alpha_8 = \frac{\langle 45\rangle}{\langle 46\rangle}
\end{aligned}$$

with a factor of $\frac{\langle 46\rangle^3 \langle 13\rangle^3}{\langle 4|Q_{456}|1\rangle^2 \langle 6|Q_{456}|3\rangle^2}$ from solving the delta functions and a Jacobian of

$$J_a = \delta_a^{-1} = \frac{\langle 4|Q_{456}|3\rangle \langle 6|Q_{456}|1\rangle}{\langle 4|Q_{456}|1\rangle \langle 6|Q_{456}|3\rangle} \tag{5.29}$$

Using the aforementioned we can also infer the Jacobian of the diagram with the internal cycle reversed

$$J_b = \frac{\langle 4|Q_{456}|3\rangle \langle 6|Q_{456}|1\rangle}{[13] \langle 46\rangle s_{456}} \tag{5.30}$$

The form obtained is then

$$d\Omega = \frac{\langle 46\rangle^4 [13]^4}{s_{456} \langle 45\rangle \langle 56\rangle [12][23] \langle 4|Q_{456}|1\rangle \langle 6|Q_{456}|3\rangle} \left(\left[\frac{\langle 4|Q_{456}|3\rangle \langle 6|Q_{456}|1\rangle}{\langle 4|Q_{456}|1\rangle \langle 6|Q_{456}|3\rangle} \right]^{-4} + \left[\frac{\langle 4|Q_{456}|3\rangle \langle 6|Q_{456}|1\rangle}{[13] \langle 46\rangle s_{456}} \right]^{-4} \right) \tag{5.31}$$

We will now analyze the singularity structure of this diagram, by assigning loop momenta to the three loops and putting the internal propagators on-shell.

5.7 Singularities

To find the singularity structure of the form obtained, we first assign the three loop momenta ℓ_1, ℓ_2 , and ℓ_3 , in the following way

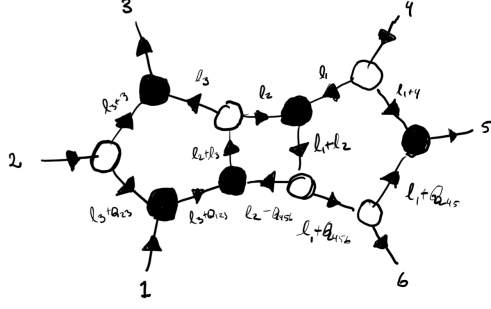


Figure 11. Six point NMHV 4+4 diagram with assigned loop momenta

We then put the internal propagators on shell, which gives the following solutions for the internal momenta

$$\begin{aligned}
\ell_1 &= \frac{\tilde{\lambda}_4}{\langle 46 \rangle} \langle 6|Q_{456}|\cdot], & \ell_2 &= \frac{1}{\langle 6|Q_{456}|1]} \langle 6|Q_{456}|\cdot] \langle \cdot|Q_{456}|1], & \ell_3 &= \frac{\tilde{\lambda}_3}{[13]} \langle \cdot|Q_{456}|1], \\
\ell_1 + 4 &= \frac{\langle 56 \rangle}{\langle 46 \rangle} \lambda_4 \tilde{\lambda}_5, & \ell_2 + \ell_3 &= \frac{\langle 6|Q_{456}|3]}{\langle 6|Q_{456}|1]} \langle \cdot|Q_{456}|1] \frac{\tilde{\lambda}_4}{[13]}, & \ell_3 + 3 &= -\frac{[12]}{[13]} \lambda_2 \tilde{\lambda}_3, \\
\ell_1 + Q_{45} &= \frac{\langle 45 \rangle}{\langle 46 \rangle} \lambda_6 \tilde{\lambda}_4, & \ell_2 - Q_{456} &= \frac{s_{456}}{\langle 6|Q_{456}|1]} \lambda_3 \tilde{\lambda}_4, & \ell_3 + Q_{23} &= \frac{[23]}{[13]} \lambda_2 \tilde{\lambda}_1, \\
\ell_1 + Q_{456} &= \frac{\lambda_6}{\langle 46 \rangle} \langle 4|s_{456}|\cdot], & \ell_1 + \ell_2 &= \frac{\langle 4|Q_{456}|1]}{\langle 6|Q_{456}|1]} \langle 6|Q_{456}|\cdot] \frac{\lambda_6}{\langle 46 \rangle}, & \ell_3 + Q_{123} &= \frac{\tilde{\lambda}_1}{[13]} \langle \cdot|s_{456}|3], \\
& & & & & (5.32)
\end{aligned}$$

Comparing this with the edge-variables, we have highlighted some of the common factors among them.

$$\begin{aligned}
\alpha_1 &= \frac{[23]}{[13]}, & \alpha_2 &= -\frac{[12]}{[13]}, & \alpha_3 &= -\frac{\langle 6|Q_{456}|1]}{\langle 6|Q_{456}|3]}, & \alpha_4 &= \frac{\langle 46 \rangle [13]}{\langle 6|Q_{456}|1]}, \\
\alpha_5 &= \frac{\langle 6|Q_{456}|1]}{\langle 4|Q_{456}|1]}, & \alpha_6 &= \frac{s_{456}}{\langle 6|Q_{456}|1]}, & \alpha_7 &= \frac{\langle 56 \rangle}{\langle 46 \rangle}, & \alpha_8 &= \frac{\langle 45 \rangle}{\langle 46 \rangle}
\end{aligned}$$

We see that sending $\{\alpha_1, \alpha_2, \alpha_6, \alpha_7, \alpha_8\} \rightarrow 0$ erases the corresponding edge, while the same happens by sending $\{\alpha_3, \alpha_5\} \rightarrow \infty$. Further we can identify

$$\begin{aligned}
\ell_1 &\rightarrow \infty, & \text{for } \langle 46 \rangle &\rightarrow 0, \\
\ell_2 &\rightarrow \infty, & \text{for } \langle 6|Q_{456}|1] &\rightarrow 0, \\
\ell_3 &\rightarrow \infty, & \text{for } [13] &\rightarrow 0.
\end{aligned} \tag{5.33}$$

We see that in the final form (5.31), these will contribute as higher order poles stemming from the Jacobian factors. From these equations we also see that erasing α_4 either comes from sending $[13]$ or $\langle 46 \rangle$ to 0 (which would send ℓ_1 or ℓ_3 to ∞) or from sending $\langle 6|Q_{456}|1] \rightarrow \infty$, which would erase α_3, α_5 , and α_6 as well.

Finally we will in the next section discuss how to construct higher loop, or non-reduced, on-shell diagrams.

6 Higher loops

One can get to higher loops with the same number of points by attaching two connected vertices to one of the graphs we have already considered. We will do this at four point to show how the form is constructed and then proceed to analyze one five-point three-loop diagram with no internal cycles and one with an internal cycle. Finally we analyze the singularity structure by comparing with the solution obtained by explicitly solving the on-shell constraints of the internal momenta.

6.1 2 loop four-point

At four points we can attach the two connected vertices to the four point diagram from section 3 to make the following two-loop diagram, with corresponding C-matrix

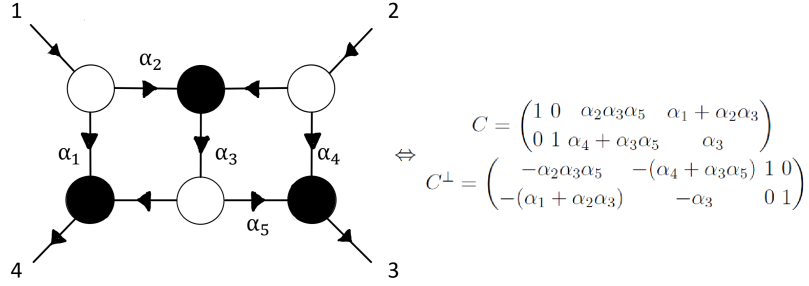


Figure 12.

Solving the bosonic delta-functions one obtains the following equations

$$\begin{aligned} 0 &= \alpha_4 \langle 12 \rangle + \alpha_3 \alpha_5 \langle 12 \rangle - \langle 13 \rangle & 0 &= \alpha_2 \alpha_3 \alpha_5 \langle 12 \rangle - \langle 23 \rangle \\ 0 &= \alpha_3 \langle 12 \rangle - \langle 14 \rangle & 0 &= -((\alpha_1 + \alpha_2 \alpha_3) \langle 12 \rangle) - \langle 24 \rangle \end{aligned} \quad (6.1)$$

Then, taking α_4 as the free parameter, we find

$$\alpha_1 = -\frac{\alpha_4 \langle 24 \rangle - \langle 34 \rangle}{\alpha_4 \langle 12 \rangle - \langle 13 \rangle}, \quad \alpha_2 = \frac{\langle 23 \rangle}{\alpha_4 \langle 12 \rangle - \langle 13 \rangle}, \quad \alpha_3 = \frac{\langle 14 \rangle}{\langle 12 \rangle}, \quad \alpha_5 = -\frac{\alpha_4 \langle 12 \rangle - \langle 13 \rangle}{\langle 14 \rangle}, \quad (6.2)$$

So that the $\mathcal{N} = 0$ form, after multiplying by the delta function Jacobian $\frac{\langle 12 \rangle^2}{\langle 14 \rangle (\alpha_4 \langle 12 \rangle - \langle 13 \rangle)}$, is

$$d\Omega = \frac{\langle 12 \rangle^4}{\alpha_4 \langle 12 \rangle \langle 23 \rangle \langle 41 \rangle (\alpha_4 \langle 24 \rangle - \langle 34 \rangle)} \delta(P) \quad (6.3)$$

Before we approach a diagram with an internal cycle, we will first give another example of a higher loop diagram, specifically at five points.

6.2 Three loop five-point in $\mathcal{N} = 0$, no internal cycle

Just like in the four-point example we can add a connected pair of vertices to one of the five point diagrams, to get a three loop graph. An example of such a graph is shown below

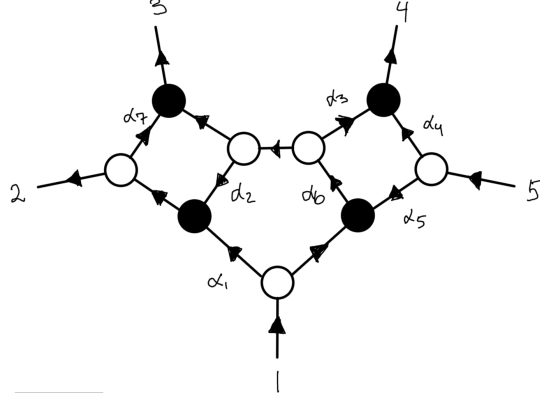


Figure 13. Three loop five-point diagram with no cycles

The on-shell condition imposed on the three loop momenta leaves us with $3 \times 4 - 11 = 1$ unfixed parameter. The C-matrices are

$$C = \begin{pmatrix} 1 & \alpha_1 + \alpha_2\alpha_6 & \alpha_2\alpha_7\alpha_6 + \alpha_6 + \alpha_1\alpha_7 & \alpha_3\alpha_6 & 0 \\ 0 & \alpha_2\alpha_5\alpha_6 & \alpha_5\alpha_6(\alpha_2\alpha_7 + 1) & \alpha_4 + \alpha_3\alpha_5\alpha_6 & 1 \end{pmatrix}$$

$$C_\perp = \begin{pmatrix} -\alpha_1 - \alpha_2\alpha_6 & 1 & 0 & 0 & -\alpha_2\alpha_5\alpha_6 \\ -\alpha_6 - (\alpha_1 + \alpha_2\alpha_6)\alpha_7 & 0 & 1 & 0 & -\alpha_5\alpha_6(\alpha_2\alpha_7 + 1) \\ -\alpha_3\alpha_6 & 0 & 0 & 1 & -\alpha_4 - \alpha_3\alpha_5\alpha_6 \end{pmatrix} \quad (6.4)$$

With the following corresponding equations stemming from the delta function

$$\delta(C_\perp \cdot \lambda) \rightarrow \begin{cases} 0 & = -\langle 12 \rangle + \alpha_2\alpha_5\alpha_6\langle 15 \rangle \\ 0 & = -((\alpha_1 + \alpha_2\alpha_6)\langle 15 \rangle) + \langle 25 \rangle \\ 0 & = -\langle 13 \rangle + \alpha_5\alpha_6(1 + \alpha_2\alpha_7)\langle 15 \rangle \\ 0 & = -((\alpha_6 + \alpha_1\alpha_7 + \alpha_2\alpha_6\alpha_7)\langle 15 \rangle) + \langle 35 \rangle \\ 0 & = -\langle 14 \rangle + (\alpha_4 + \alpha_3\alpha_5\alpha_6)\langle 15 \rangle \\ 0 & = -(\alpha_3\alpha_6\langle 15 \rangle) + \langle 45 \rangle \end{cases} \quad (6.5)$$

It is natural choice in this case to take either α_7 or α_4 as the free parameters. We take α_7 and note that since removing α_7 gives us one of the five-point graphs analyzed earlier in this report, one would expect the residue at $\alpha_7 = 0$ of the resulting form to match the five-point two loop result. Solving the delta-functions we find

$$\alpha_1 = -\frac{\langle 23 \rangle}{\alpha_7\langle 12 \rangle - \langle 13 \rangle}, \quad \alpha_2 = -\frac{\langle 12 \rangle}{\alpha_7\langle 12 \rangle - \langle 13 \rangle}, \quad \alpha_3 = -\frac{\langle 45 \rangle}{\alpha_7\langle 25 \rangle - \langle 35 \rangle}$$

$$\alpha_4 = -\frac{\alpha_7\langle 24 \rangle - \langle 34 \rangle}{\alpha_7\langle 25 \rangle - \langle 35 \rangle}, \quad \alpha_5 = \frac{\alpha_7\langle 12 \rangle - \langle 13 \rangle}{\alpha_7\langle 25 \rangle - \langle 35 \rangle}, \quad \alpha_6 = -\frac{\alpha_7\langle 25 \rangle - \langle 35 \rangle}{\langle 15 \rangle} \quad (6.6)$$

Such that

$$\begin{aligned}
& \delta(C_\perp \cdot \lambda) \delta(C \cdot \tilde{\lambda}) \\
&= \frac{\langle 15 \rangle^3}{(\alpha_7 \langle 12 \rangle - \langle 13 \rangle)(-\alpha_7 \langle 25 \rangle + \langle 35 \rangle)^2} \delta^4(P) \delta \left(\alpha_1 + \frac{\langle 23 \rangle}{\alpha_7 \langle 12 \rangle - \langle 13 \rangle} \right) \delta \left(\alpha_2 + \frac{\langle 12 \rangle}{\alpha_7 \langle 12 \rangle - \langle 13 \rangle} \right) \\
& \quad \delta \left(\alpha_3 + \frac{\langle 45 \rangle}{\alpha_7 \langle 25 \rangle - \langle 35 \rangle} \right) \delta \left(\alpha_4 + \frac{\alpha_7 \langle 24 \rangle - \langle 34 \rangle}{\alpha_7 \langle 25 \rangle - \langle 35 \rangle} \right) \delta \left(\alpha_5 - \frac{\alpha_7 \langle 12 \rangle - \langle 13 \rangle}{\alpha_7 \langle 25 \rangle - \langle 35 \rangle} \right) \delta \left(\alpha_6 + \frac{\alpha_7 \langle 25 \rangle - \langle 35 \rangle}{\langle 15 \rangle} \right), \\
& \hspace{15em} (6.7)
\end{aligned}$$

and we get the form

$$d\Omega = \frac{\langle 15 \rangle^4}{\alpha_7 \langle 12 \rangle \langle 23 \rangle \langle 45 \rangle \langle 15 \rangle (\alpha_7 \langle 24 \rangle - \langle 34 \rangle)}. \quad (6.8)$$

Taking the residue of the form at $\alpha_7 = 0$ one recovers the standard YM Parke-Taylor tree-level amplitude, as expected.

$$d\Omega = \frac{\langle 15 \rangle^4}{\langle 12 \rangle \langle 23 \rangle \langle 34 \rangle \langle 45 \rangle \langle 51 \rangle} \quad (6.9)$$

Further, we note that the form has one other pole at $\alpha_7 = \frac{\langle 34 \rangle}{\langle 24 \rangle}$. Since we now have an intuition for the procedure, let us repeat this for a diagram with an internal cycle.

6.3 Three loop five-point in $\mathcal{N} = 0$ with internal cycle

We will consider the following graph

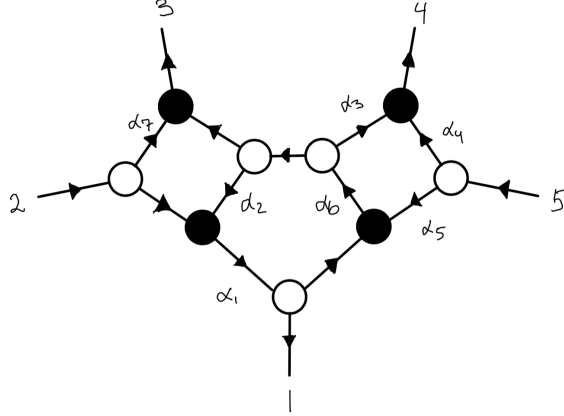


Figure 14. Diagram A: three loop, five point

To get form of the cut, one has to fix the helicity configuration and then find all the configurations of the internal momenta that yield a perfect orientation. The only other possible diagram would have the internal cycle going clockwise instead; we will refer to that as diagram *B*. Since the bare form is the same for both diagrams, the only point of difference is the Jacobians.

For diagram A, the C-matrices are

$$C = \begin{pmatrix} \alpha_1 \delta_a & 1 & \alpha_1 \alpha_6 \delta_a + \alpha_7 & \alpha_1 \alpha_3 \alpha_6 \delta_a & 0 \\ \alpha_1 \alpha_2 \alpha_5 \alpha_6 \delta_a & 0 & \alpha_5 \alpha_6 \delta_a & \alpha_3 \alpha_5 \alpha_6 \delta_a + \alpha_4 & 1 \end{pmatrix}$$

$$C_\perp = \begin{pmatrix} 1 & -\alpha_1 \delta_a & 0 & 0 & -\alpha_1 \alpha_2 \alpha_5 \alpha_6 \delta_a \\ 0 & -\alpha_1 \alpha_6 \delta_a - \alpha_7 & 1 & 0 & -\alpha_5 \alpha_6 \delta_a \\ 0 & -\alpha_1 \alpha_3 \alpha_6 \delta_a & 0 & 1 & -\alpha_3 \alpha_5 \alpha_6 \delta_a - \alpha_4 \end{pmatrix}, \quad (6.10)$$

where $\delta_a = \frac{1}{1 - \alpha_1 \alpha_2 \alpha_6}$. The first delta-function constraint gives us

$$\delta^6(C_\perp \cdot \lambda) \rightarrow \begin{cases} 0 & = \langle 12 \rangle + \alpha_1 \alpha_2 \alpha_5 \alpha_6 \delta_a \langle 25 \rangle \\ 0 & = \langle 15 \rangle - \alpha_1 \delta_a \langle 25 \rangle \\ 0 & = -\langle 23 \rangle + \alpha_5 \alpha_6 \delta_a \langle 25 \rangle \\ 0 & = (-\alpha_7 - \alpha_1 \alpha_6 \delta_a) \langle 25 \rangle + \langle 35 \rangle \\ 0 & = -\langle 24 \rangle - (-\alpha_4 - \alpha_3 \alpha_5 \alpha_6 \delta_a) \langle 25 \rangle \\ 0 & = -(\alpha_1 \alpha_3 \alpha_6 \delta_a \langle 25 \rangle) + \langle 45 \rangle \end{cases} \quad (6.11)$$

Solving the delta-functions we find

$$\begin{aligned} \alpha_1 &= -\frac{\alpha_7 \langle 12 \rangle - \langle 13 \rangle}{\langle 23 \rangle}, & \alpha_2 &= -\frac{\langle 12 \rangle}{\alpha_7 \langle 12 \rangle - \langle 13 \rangle}, & \alpha_3 &= -\frac{\langle 45 \rangle}{\alpha_7 \langle 25 \rangle - \langle 35 \rangle} \\ \alpha_4 &= -\frac{\alpha_7 \langle 24 \rangle - \langle 34 \rangle}{\alpha_7 \langle 25 \rangle - \langle 35 \rangle}, & \alpha_5 &= \frac{\alpha_7 \langle 12 \rangle - \langle 13 \rangle}{\alpha_7 \langle 25 \rangle - \langle 35 \rangle}, & \alpha_6 &= -\frac{\alpha_7 \langle 25 \rangle - \langle 35 \rangle}{\langle 15 \rangle} \\ \delta_a &= -\frac{\langle 15 \rangle \langle 23 \rangle}{\langle 25 \rangle (\alpha_7 \langle 12 \rangle - \langle 13 \rangle)} \end{aligned} \quad (6.12)$$

$$\begin{aligned} & \delta(C_\perp \cdot \lambda) \delta(C \cdot \tilde{\lambda}) \\ &= \frac{\langle 15 \rangle^4 (\alpha_7 \langle 12 \rangle - \langle 13 \rangle)}{\langle 15 \rangle^2 \langle 23 \rangle^2 (-\alpha_7 \langle 25 \rangle + \langle 35 \rangle)^2} \delta^4(P) \delta \left(\alpha_1 + \frac{\alpha_7 \langle 12 \rangle - \langle 13 \rangle}{\langle 23 \rangle} \right) \delta \left(\alpha_2 + \frac{\langle 12 \rangle}{\alpha_7 \langle 12 \rangle - \langle 13 \rangle} \right) \\ & \delta \left(\alpha_3 + \frac{\langle 45 \rangle}{\alpha_7 \langle 25 \rangle - \langle 35 \rangle} \right) \delta \left(\alpha_4 + \frac{\alpha_7 \langle 24 \rangle - \langle 34 \rangle}{\alpha_7 \langle 25 \rangle - \langle 35 \rangle} \right) \delta \left(\alpha_5 - \frac{\alpha_7 \langle 12 \rangle - \langle 13 \rangle}{\alpha_7 \langle 25 \rangle - \langle 35 \rangle} \right) \delta \left(\alpha_6 + \frac{\alpha_7 \langle 25 \rangle - \langle 35 \rangle}{\langle 15 \rangle} \right) \end{aligned} \quad (6.13)$$

The bare form matches that of our earlier diagram (albeit with a different helicity structure)

$$d\Omega_{\text{bare}} = \frac{\langle 25 \rangle^4}{\alpha_7 \langle 12 \rangle \langle 51 \rangle \langle 23 \rangle \langle 45 \rangle (\alpha_7 \langle 24 \rangle - \langle 34 \rangle)} \quad (6.14)$$

and we note that taking the residue of the form at $\alpha_7 = 0$ one recovers the standard YM Parke-Taylor tree-level amplitude

$$\frac{\langle 25 \rangle^4}{\langle 12 \rangle \langle 23 \rangle \langle 34 \rangle \langle 45 \rangle \langle 51 \rangle} \quad (6.15)$$

To get the form of the cut we find that the Jacobian is

$$J_a = \delta_a^{-1} = \frac{\langle 25 \rangle (\alpha_7 \langle 12 \rangle - \langle 13 \rangle)}{\langle 15 \rangle \langle 23 \rangle} \quad (6.16)$$

While the Jacobian for the diagram with the internal cycle in the opposite direction is

$$J_b = \frac{\langle 25 \rangle (\alpha_7 \langle 12 \rangle - \langle 13 \rangle)}{\langle 12 \rangle (\alpha_7 \langle 25 \rangle - \langle 35 \rangle)} \quad (6.17)$$

Which gives the total $\mathcal{N} = 0$ form

$$d\Omega = \frac{\langle 25 \rangle^4}{\alpha_7 \langle 12 \rangle \langle 51 \rangle \langle 23 \rangle \langle 45 \rangle (\alpha_7 \langle 24 \rangle - \langle 34 \rangle)} \left(\left[\frac{\langle 25 \rangle (\alpha_7 \langle 12 \rangle - \langle 13 \rangle)}{\langle 15 \rangle \langle 23 \rangle} \right]^{-4} + \left[\frac{\langle 25 \rangle (\alpha_7 \langle 12 \rangle - \langle 13 \rangle)}{\langle 12 \rangle (\alpha_7 \langle 25 \rangle - \langle 35 \rangle)} \right]^{-4} \right) \quad (6.18)$$

6.4 Singularities

To look at the singularity structure of the five-point three-loop on-shell diagram, we once again look at

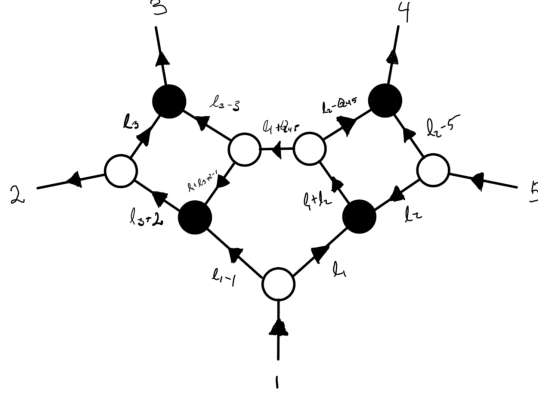


Figure 15. Three-loop diagram with loop momenta assigned.

Where we have assigned 3 different loop-momenta, ℓ_1 , ℓ_2 , and ℓ_3 . The momenta is found to be

$$\begin{aligned} \ell_3 &= \lambda_2 \tilde{\lambda}_3, & \ell_3 + 2 &= \lambda_2 (z \tilde{\lambda}_3 - \tilde{\lambda}_2), & \ell_3 - 3 &= \tilde{\lambda}_3 (z \lambda_2 + \lambda_3) \\ \ell_1 &= \frac{\lambda_1}{z \langle 12 \rangle - \langle 13 \rangle} (z \langle 2 | Q_{123} | \cdot \rangle - \langle 3 | Q_{123} | \cdot \rangle), & \ell_2 &= -\frac{\lambda_5}{z \langle 25 \rangle - \langle 35 \rangle} (z \langle 2 | Q_{123} | \cdot \rangle - \langle 3 | Q_{123} | \cdot \rangle) \\ \ell_2 - 5 &= \frac{z \langle 24 \rangle - \langle 34 \rangle}{z \langle 25 \rangle - \langle 35 \rangle} \lambda_5 \tilde{\lambda}_4, & \ell_2 - Q_{45} &= \frac{\langle 45 \rangle}{z \langle 25 \rangle - \langle 35 \rangle} \tilde{\lambda}_4 (z \lambda_2 - \lambda_3) \\ \ell_1 - 1 &= \frac{\langle 23 \rangle}{z \langle 12 \rangle - \langle 13 \rangle} \lambda_1 (z \tilde{\lambda}_3 + \tilde{\lambda}_2), & \ell_1 + Q_{45} &= \frac{z \lambda_2 - \lambda_3}{z \langle 12 \rangle - \langle 13 \rangle} (\langle 12 \rangle \tilde{\lambda}_2 + z \langle 12 \rangle \tilde{\lambda}_3 - \langle 13 \rangle \tilde{\lambda}_3) \end{aligned} \quad (6.19)$$

$$\begin{aligned}
\ell_1 + \ell_2 &= \frac{\langle 15 \rangle (z\lambda_2 - \lambda_3)}{(z\langle 12 \rangle - \langle 13 \rangle)(z\langle 25 \rangle - \langle 35 \rangle)} (z\langle 2|Q_{123}|\cdot\rangle - \langle 3|Q_{123}|\cdot\rangle) \\
\ell_1 + \ell_3 + 2 - 1 &= \frac{\langle 12 \rangle}{z\langle 13 \rangle - \langle 12 \rangle} (z\lambda_2 - \lambda_3) (z\tilde{\lambda}_3 - \tilde{\lambda}_2)
\end{aligned} \tag{6.20}$$

First we note that after identifying $z = -\alpha_7$ the $\mathcal{N} = 4$ form found by combining three-point amplitudes using the momenta above, matches the results obtained in the previous sections

$$d\Omega_5 = \frac{\delta(P)\delta(Q)}{z\langle 12 \rangle \langle 23 \rangle \langle 45 \rangle \langle 51 \rangle (z\langle 24 \rangle + \langle 34 \rangle)} \tag{6.21}$$

Further we see that the $\ell_2 - 5$ coefficient directly corresponds to the α_4 edge, and below we have highlighted the common factors.

$$\begin{aligned}
\alpha_1 &= -\frac{\langle 23 \rangle}{\alpha_7 \langle 12 \rangle - \langle 13 \rangle}, & \alpha_2 &= -\frac{\langle 12 \rangle}{\alpha_7 \langle 12 \rangle - \langle 13 \rangle}, & \alpha_3 &= -\frac{\langle 45 \rangle}{\alpha_7 \langle 25 \rangle - \langle 35 \rangle} \\
\alpha_4 &= -\frac{\alpha_7 \langle 24 \rangle - \langle 34 \rangle}{\alpha_7 \langle 25 \rangle - \langle 35 \rangle}, & \alpha_5 &= \frac{\alpha_7 \langle 12 \rangle - \langle 13 \rangle}{\alpha_7 \langle 25 \rangle - \langle 35 \rangle}, & \alpha_6 &= -\frac{\alpha_7 \langle 25 \rangle - \langle 35 \rangle}{\langle 15 \rangle}
\end{aligned} \tag{6.22}$$

Comparing Figure 13 and Figure 14 with their respective edge-variables, one sees that flipping arrows inside the diagram inverts the corresponding edge-variable. Sending one of $\{\alpha_1, \alpha_2, \alpha_3, \alpha_4, \alpha_5\} \rightarrow 0$ sends the corresponding edge to zero, while $\alpha_6 \rightarrow \infty$ erases that edge. This agrees with the statement found at six points that edges that contain an arrow from a white to a black vertex is erasable by sending $\alpha \rightarrow 0$ and from black to white by $\alpha \rightarrow \infty$. Finally, sending $\ell_1 \rightarrow \infty$ gives a higher order pole in the form for the cut.

7 Summary and outlook

In this report we first gave a brief introduction to the Grassmannian and on-shell diagrams. We then outlined how to get $\mathcal{N} = 4$ sYM amplitudes from these, by explicitly calculating examples at four, five, and six points. The techniques were then extended to $\mathcal{N} \neq 4$ by considering all internal configurations for a specific fixed external helicity configuration, specifically focusing on $\mathcal{N} = 0$. When diagrams contain an internal cycle, a Jacobian contributes, and the form does not give the amplitudes but rather represent cuts of loop integrands, while the *bare* form, (i.e. the form without the Jacobian), gave the normal MHV Parke-Taylor amplitudes.

We then considered the singularity structure by comparing the form and corresponding edge-variables with the diagram's loop-variables, found by explicitly putting the internal propagators on-shell. The six point NMHV on-shell form considered has higher order poles when the loop momenta goes to infinity. Further we saw that the edge-variables erase an edge by going to 0 when the arrow points from a white to a black vertex, while the edge is erased for the variable going to ∞ for arrows pointing from black to white vertices.

Finally we looked at higher loop diagrams at four- and five-point, i.e. having one parameter unfixed. Here we found that a higher order poles arises when the pentagon loop momenta goes to infinity. The residues of the forms at these poles are yet to be analyzed, while explicitly computing forms at other \mathcal{N} , along with their residues when the loop momenta goes to infinity, provides more avenues that can be pursued.

References

- [1] N. Arkani-Hamed, J. L. Bourjaily, F. Cachazo, S. Caron-Huot and J. Trnka, JHEP **01**, 041 (2011) doi:10.1007/JHEP01(2011)041 [arXiv:1008.2958 [hep-th]].
- [2] H. Elvang and Y. t. Huang, “Scattering Amplitudes in Gauge Theory and Gravity,”
- [3] N. Arkani-Hamed and J. Trnka, JHEP **10**, 030 (2014) doi:10.1007/JHEP10(2014)030 [arXiv:1312.2007 [hep-th]].
- [4] N. Arkani-Hamed and J. Trnka, JHEP **12**, 182 (2014) doi:10.1007/JHEP12(2014)182 [arXiv:1312.7878 [hep-th]].
- [5] N. Arkani-Hamed, A. Hodges and J. Trnka, JHEP **08**, 030 (2015) doi:10.1007/JHEP08(2015)030 [arXiv:1412.8478 [hep-th]].
- [6] N. Arkani-Hamed, J. L. Bourjaily, F. Cachazo, A. Postnikov and J. Trnka, JHEP **06**, 179 (2015) doi:10.1007/JHEP06(2015)179 [arXiv:1412.8475 [hep-th]].
- [7] N. Arkani-Hamed, J. L. Bourjaily, F. Cachazo, A. B. Goncharov, A. Postnikov and J. Trnka, doi:10.1017/CBO9781316091548 [arXiv:1212.5605 [hep-th]].
- [8] E. Herrmann and J. Trnka, JHEP **11**, 136 (2016) doi:10.1007/JHEP11(2016)136 [arXiv:1604.03479 [hep-th]].